Sensitivity analysis, calibration and validation of a phenology model for *Pityogenes chalcographus* (CHAPY)

Nikica Ogris [a,*], Mitja Ferlan [a], Tine Hauptman [b], Roman Pavlin [b], Andreja Kavčič [a], Maja Jurc [b], Maarten de Groot [a]

[a] Slovenian Forestry Institute, Večna pot 2, 1000 Ljubljana, Slovenia

[b] Department of Forestry and Renewable Forest Resources, Biotechnical Faculty, University of Ljubljana, Večna pot 83, 1000 Ljubljana, Slovenia

* Corresponding author. E-mail address: nikica.ogris@gozdis.si (N. Ogris).

Abstract

The purpose of the study was to develop, calibrate and validate a comprehensive phenological model for the spatiotemporal simulation of the seasonal development of the six-toothed spruce bark beetle, *Pityogenes chalcographus* (CHAPY). The validation dataset was acquired through monitoring of the bark beetle's phenology at eight sites in Slovenia in 2017 and 2018, along with air and bark temperature measurements. The predictions were made using air temperature from the INCA system (Integrated Nowcasting through Comprehensive Analysis), which is used to calculate the effective bark temperature for beetle development. Since the biology of *P. chalcographus* is poorly studied, a sensitivity analysis was used to pinpoint the most important model parameters. The first order (main) effect was the highest for the lower developmental threshold (DT_L), while the second order (interaction, total) effect was the highest for the optimum temperature (*To*). DT_L was calibrated with an iterative procedure, and the best result with the lowest mean absolute error (MAE) was achieved at 7.4°C. Effective temperatures in the range between *To* and the upper developmental threshold were calculated with a nonlinear function whose parameters were appropriately calibrated. The spring date threshold when the model calculation starts was calibrated with an iterative procedure and set at 9th March, which had the minimum MAE. The onset of Norway spruce infestation in spring was estimated using a lower threshold of 15.6°C for flight activity and a mean thermal sum of 216.5 degree-days (dd) from 9th March onward. The observed mean thermal sum required for total development of filial beetles was 652.8 ± 22.7°C, while the predicted mean thermal sum was 635.4 ± 31.4°C. Re-emergence of parental beetles occurred when 52.7% of the minimum thermal sum for total development was reached. The relative duration of the egg, larval and combination of the pupal and teneral adult developmental stages was 9.4%, 58.2% and 32.4%, respectively. Mass swarming concluded in the end of August when daylength was lower than 13.6 h, which was determined with the independent dataset of 1,017 pheromone traps. The diapause initiation at a daylength < 13.6 h is included in the model as an assumption. Successful hibernation of established broods is predicted by assessing the developmental stage of initiated generations at the 31st December. For validation, we compared the timing of phenological events in the field with predicted events using both 30-minute recorded data at study sites in the field and hourly data from the INCA. The time of spring swarming was estimated with a MAE of 5.6 days. The onset of infestation was predicted with a MAE of 6.0 days. The predicted onset of emergence of filial beetles was estimated with a MAE of 2.1 days. Additionally, CHAPY simulates the number of generations. CHAPY was successfully incorporated into two publicly available web applications. Development of the model revealed several knowledge gaps in *P. chalcographus* phenology, thus providing opportunities for further research of the second most damaging bark beetle of Norway spruce in Central Europe and for further improvement of the CHAPY model. Potential applications of the model for monitoring and management of *P. chalcographus* are discussed.

Keywords: Six-toothed spruce bark beetle; Insect outbreak; Population dynamics; Voltinism; Ecological modelling; Pheromone trap, Trap tree, Monitoring

1. Introduction

The six-toothed spruce bark beetle, *Pityogenes chalcographus* (Linnaeus, 1761) (Coleoptera: Curculionidae, Scolytinae), is a widely distributed forest pest in Europe, infesting mainly Norway spruce (*Picea abies* (L.) H. Karst.) and also some other native European and introduced North American conifers (Avtziz *et al.*, 2010; Hedgren, 2004; Kacprzyk, 2012; Schwerdtfeger, 1929). *P. chalcographus* is commonly regarded as the second most important insect pest of Norway spruce in Central Europe after European spruce bark beetle, *Ips typographus* (Linnaeus, 1758) (Coleoptera: Scolytinae) (Göthlin *et al.*, 2000; Hedgren, 2004; Hedgren *et al.*, 2003; Kula and Ząbecki, 2006). *P. chalcographus* preferably attacks either young spruce trees or the tops and branches of older spruce trees, usually after they have suffered from previous damage caused by drought, pollutants or simultaneous attack by the *I. typographus* (Göthlin *et al.*, 2000; Hedgren, 2004; Schroeder, 2013; Zúbrik *et al.*, 2008). The relatively good capacity of *P. chalcographus* for host plant shifting and dispersal (Bertheau *et al.*, 2012; Bertheau *et al.*, 2009), together with global climatic changes that negatively affect the health status of Norway spruce stands, may result in increasing occurrence of population outbreaks of this pest in the future (Avtziz *et al.*, 2010; Heliövaara and Peltonen, 1999; Ogris and Jurc, 2010; Verkaik *et al.*, 2009).

Phenology models play an important role in insect ecology and pest management (Berec *et al.*, 2013; Damos and Savopoulou-Soultani, 2012; Depinay *et al.*, 2004; Otero *et al.*, 2008). They are indispensable tools for predicting swarming periods, thus allowing timely deployment of monitoring, e.g. by pheromone traps or trap trees (Baier *et al.*, 2007; Ogris *et al.*, 2019). Also, phenology models enable us to discern sister generations that are hard to recognize in the field and frequently disregarded in studies of bark beetle population dynamics (e.g. Fahse and Heurich, 2011) despite their significant contribution to population size (Wermelinger and Seifert, 1999). Simulation models that aim to predict bark beetle dynamics at a specific location to a sufficient degree of accuracy should thus take sister generations into account (Berec *et al.*, 2013). Additionally, phenology models tell us to what extent the diapausing bark beetles develop, which is an important factor in determining the probability that they will survive winter.

Additionally, to assess the likelihood of mass outbreaks in time, appropriate monitoring tools need to accurately predict the actual developmental process of the bark beetle population and the number of bark beetle generations per year. Such a tool or model would need to address the spatiotemporal dynamics of the bark beetle population and its temperature-dependant phenology, including timing and the number of all filial and sister generations. Although basic information on voltinism and the phenology of *P. chalcographus* is known (Coeln *et al.*, 1996; Führer and Chen, 1979; Lobinger, 1994; Zumr, 1982), a phenology model is missing. In contrast, for *I. typographus*, a comprehensive phenology model called PHENIPS has been developed and used in several countries in Central Europe (Baier *et al.*, 2012; Baier *et al.*, 2007; Berec *et al.*, 2013). PHENIPS predicts spatiotemporal dynamics, including the number and timing of all filial and sister generations and the actual developmental process of the *I. typographus* population. PHENIPS was validated, calibrated for a new geographical region (Slovenia) and appropriately changed. Through this process, the RITY-2 model was developed (Ogris *et al.*, 2019). RITY-2 was successfully incorporated into two web applications that serve as tools for the timely deployment of pheromone traps and trap trees for monitoring of *I. typographus* population abundance (Ogris, 2018a, b).

The purpose of this study was to develop, calibrate and validate a phenology model of *P. chalcographus*. We used RITY-2 as a framework on which we developed a phenological model called CHAPY (acronym for CHAlcographus PitYogenes).

2. Material and methods

2.1. Area description

Approximately 58% of Slovenia is covered with forests (ZGS, 2018b). Although Slovenia is relatively small in area, it is comprised of the Alpine, pre-Alpine, Dinaric, pre-Dinaric, pre-Pannonian and pre-Mediterranean biogeographical regions, all of which have their own climatic

conditions and typical forest habitat types (Zupančič *et al.*, 1987). The most common tree species is European beech (*Fagus sylvatica* L.), followed by Norway spruce. Norway spruce is most abundant in the Alpine, pre-Alpine, Dinaric and pre-Dinaric regions.

In the last twenty years, Slovenia has experienced two large epidemic periods of spruce bark beetle outbreaks (de Groot and Ogris, 2019). One period started in 2003 during extremely warm and dry climatic conditions, and this epidemic period continued until 2008. After this period, sanitary felling was higher than that in the period before the 2003 drought. The years 2012 and 2013 were very dry, and there was a noticeable increase in sanitary felling of Norway spruce because of bark beetles. However, in 2014 there was a large-scale ice storm that affected 9.3 Mio. m^3 of trees (ZGS, 2018b). Although a larger proportion of deciduous trees were affected than coniferous trees (Nagel *et al.*, 2016), many spruce trees were damaged (de Groot *et al.*, 2018). This could be one of the reasons why sanitary felling increased dramatically because of bark beetle outbreaks (de Groot *et al.*, 2018). Between 2014 and 2017, 7.1 Mio. m^3 of Norway spruce were sanitary felled due to bark beetles as a response to the damage caused by the ice storm in 2014 (ZGS, 2018c). In December 2017, 2.2 Mio. m^3 of trees were felled by a catastrophic windthrow event, which damaged mostly conifers (90%) (ZGS, 2018a). Therefore, there is an increased risk of *P. chalcographus* outbreaks, which is a common occurrence after such events (Göthlin *et al.*, 2000; Kacprzyk, 2012).

2.2. Modelling workflow

The modelling procedure was performed in the following order: (1) Field studies were set up to acquire data for model validation and calibration; (2) A sensitivity analysis of daily effective thermal sum was performed; (3) Calibration of the model parameters; (3.1) Calibration of the lower developmental threshold; (3.2) Calibration of the effective temperature above the optimal temperature; (3.3.) Calibration of the spring date threshold from which calculation of the model is initiated; (3.4) Calibration of the end of mass swarming; (4) Model validation; (4.1) Validation of daily and cumulative effective thermal sums; (4.2) Validation of maximum air temperature at which flight activity initiates; (4.3) Validation of thermal sums needed for onset of swarming and onset of tree colonization; (4.4) Validation of brood development rate; (4.5) Validation of duration of developmental stages; (4.6) Validation of re-emergence of parental beetles, i.e. development of sister broods.

2.3. Field studies

Field experiments were conducted on the same study sites used for RITY-2 (Ogris *et al.*, 2019): at the southern edge of the Kamnik–Savinja Alps in 2017, in the south-eastern hills of the Ljubljana Marshes in the Dinaric Alps in 2018, and in the vicinity of Lake Bled in 2018. The timing of spring swarming of *P. chalcographus* was recorded during two consecutive years (2017–2018) using flight-barrier traps (WitaTrap®, Witasek PflanzenSchutz GmbH, Feldkirchen in Kärnten, Austria) baited with Chalcoprax® (BASF SE, Ludwigshafen, Germany). The traps (one per site) were placed at four sites in 2017 (Vodice, Kamnik, Brode and Prevala) and five sites in 2018 (Medvedica, Turjak, Erjavčev laz, Mokrc and Vorenčkojca) at different elevations (Table 1). We counted the number of captured beetles at two- to three-day intervals.

To observe the onset of tree colonization and brood development, we used eight trap logs (pruned trap trees) at eight different sites in 2017 and 2018 (one trap log per site) (Table 1). The length of the trap logs ranged from 12.8 to 35.0 m (average 28.2 m), and diameter at breast height ranged from 21 to 46 cm (average 35 cm). The trap logs were placed under the canopy in shade to half shade conditions. We inspected every trap log for the possible presence of overwintering beetles; no entrance holes were found in freshly felled logs. At weekly intervals, newly bored entrance holes were identified by fresh frass and marked with coloured tacks and numbered consecutively. At the same time, breeding systems under the marked entrance holes were inspected by removing pieces of bark. The most advanced developmental stage of offspring was recorded. As soon as the brood reached the pupal stage, two to three chunks with different onsets of infestation (length 40–70 cm) were removed from the trap log and transferred into two plant growth chambers (RK-1000 CH,

Kambič d.o.o., Semič, Slovenia) for daily observation of emerging filial beetles. In the first plant growth chamber, logs were kept at 23.0 ± 0.3°C, 70% relative humidity and long-day photoperiods of 16 h light and 8 h dark. Settings in the second chamber were identical except for temperature, which was set to 28.0 ± 0.3°C. The actual temperature and relative humidity in each of the plant growth chambers were recorded with two sensors at 30-min interval (Voltcraft DL-120TH, Conrad Electronic SE, Germany). Daily observation of emerging filial beetles at two different temperatures in plant growth chambers effectively doubled the sample size and enabled validation of the cumulative thermal sum of effective temperatures for the total development of *P. chalcographus* with high accuracy.

Relative air humidity and air temperature at the pheromone trap and trap log sites were recorded at 30-min intervals using SHT21 sensors (Sensirion AG, Switzerland) placed into a solar radiation shield 2 m above the ground. Likewise, we recorded bark temperature at 30-min intervals at the crown base of each trap log at four positions around the trunk (top, bottom, and lateral sides) using thermistor sensors (NTCLE305E4103SB, Vishay Intertechnology, Inc.). All sensors were connected to a compact and multi-purpose FTP data logger (Laboratory for Electronic devices, Slovenian Forestry Institute, Slovenia). The data were transferred automatically via GPRS signal and were thus available in real time using the eEMIS-SFI web application (AMES d.o.o and Slovenian Forestry Institute, Slovenia).

Table 1: Location, elevation, aspect and slope for each trap log, with the date of felling

Location	Elevation (m a.s.l.)	Longitude (°East)	Latitude (°North)	Aspect	Slope (°)	Date of felling	Year of monitoring
Vodice	330	14.53352	46.18860	Flat	3	10/3/2017	2017
Kamnik	578	14.62817	46.21906	NNE	15	10/3/2017	2017
Brode	830	14.76272	46.24221	WNW	32	12/3/2017	2017
Prevala	1038	14.75218	46.24833	Flat	6	12/3/2017	2017
Medvedica	426	14.62660	45.90970	WNW	7	22/3/2018	2018
Turjak	510	14.61615	45.86659	SSW	7	22/3/2018	2018
Erjavčev laz	849	14.50619	45.88600	SW	23	19/4/2018	2018
Mokrc	1016	14.52877	45.89407	ESE	10	19/4/2018	2018
Vorenčkojca*	578	13.88658	46.29071	SE	7		2018

* Only the pheromone trap was monitored at the location.

2.4. Modelling temperatures

The climatic model used was identical to that used for RITY-2 (Ogris *et al.*, 2019). The same procedures for air temperature and bark temperature were used for CHAPY (Eqs. (A.1)–(A.6)). However, there were differences in the calculation of daily effective thermal sums.

The air temperature 2 m above the ground was measured at every study site every 30 min as explained in section 2.3. In the application of the CHAPY model, interpolated air temperature from the INCA system was used (Haiden *et al.*, 2011; Kann *et al.*, 2012; Ogris, 2017a, b). Analysis and nowcasting contains several meteorological parameters, of which we used only air temperature 2 m above the ground. The update frequency of air temperature from the INCA system is one hour. Minimum, mean and maximum daily air temperatures from the INCA system were used in the CHAPY model. The linear regression models for minimum, mean and maximum daily air temperatures in the forest stand were calculated using measured air temperature in the forest stands from study sites as the target variable and interpolated air temperature from the INCA system as the source variable. Estimates of minimum, mean and maximum daily air temperatures in the forest stand were then calculated using the appropriate regression coefficients (Eqs. (A.1)–(A.3)) (Ogris *et al.*, 2019).

We recorded the bark temperature at the crown base of each of the eight trap logs at four positions around the trunk (top, bottom and lateral sides) at a time interval of 30 min. To estimate daily minimum, mean and maximum bark temperatures, we used linear regression analysis with observed

air temperature as the source variable and measured bark temperature as the target variable. Estimates of minimum, mean and maximum daily bark temperatures in the forest stand were then calculated using the appropriate regression coefficients (Eqs. (A.4)–(A.6)) (Ogris *et al.*, 2019).

The daily and cumulative effective thermal sums for bark beetle development were calculated from the difference between the daily mean bark temperature and the lower developmental threshold (DT_L) within the range of DT_L and optimum temperature (T_O). To avoid overestimating the effective thermal sum at bark temperatures between T_O and the upper developmental threshold (DT_U), we corrected the estimated daily thermal sums by calculating the effective bark temperature sum of a nonlinear model (Eq. 5).

The daily and cumulative effective thermal sums were calculated. The daily effective thermal sum was calculated from the observed bark temperature, recorded every 30 min. For validation of the thermal sums, we used the estimated bark temperature calculated by the formulas available from RITY-2 (Eqs. (A.4)–(A.6)) (Ogris *et al.*, 2019). The cumulative effective thermal sum was calculated over the entire study period of measuring effective bark temperatures in the field.

2.5. Sensitivity analysis of the daily effective thermal sum

Two different sensitivity indexes describing the proportion of variance of the procedure for calculation of effective temperature (Y) explained by the variation of a given parameter X_i were calculated using the Sobol'-Jansen method implemented in the "sensitivity" package of the R software program (Iooss *et al.*, 2019). The Sobol'-Jansen method implements Monte Carlo estimation of the variance-based method for sensitivity analysis proposed by Sobol' (1993) and later improved by Jansen (1999) and Saltelli *et al.* (2010). More precisely, these functions allow the estimation of the first order (main effect) and total effect indices from the variance decomposition. The main effect index is defined as:

$$S_i = \frac{Var_{Xi}(E_{X\sim i}(Y|X_i))}{Var(Y)} \quad (1)$$

with

$$\sum_{i=1}^{n} S_i = 1 \quad (S_i > 0) \quad (2)$$

Y is the prediction and X_i is the ith parameter of the procedure for calculation of effective temperature (DT_L, T_O, DT_U). The notation ($X\sim i$) indicates the set of all variables except X_i. The numerator represents the contribution of the main effect of X_i to the variation in the output, i.e. the effect of varying X_i alone, but average over variations in other input parameters. S_i is standardized by the total variance to provide the fractional contribution of each parameter i.

The total effect index is defined as:

$$S_{Ti} = \frac{E_{X\sim i}\left(Var_{Xi}(Y|X_{\sim i})\right)}{Var(Y)} = 1 - \frac{Var_{X\sim i}\left(E_{Xi}(Y|X_{\sim i})\right)}{Var(Y)} \quad (3)$$

with

$$\sum_{i=1}^{n} S_{Ti} \geq 1 \quad (S_{Ti} > 0) \quad (4)$$

S_{Ti} measures the contribution of X_i to the variation in the output, including all variances caused by its interactions with any other input variables.

With the sensitivity analysis, we tested main and total effect on the variance of the three parameters for calculating effective temperature, i.e. DT_L, T_O and DT_U. The sensitivity analysis was performed with 12,000 parameter combinations. We used uniform distribution for two random samples (N = 2,000). The bounds of the sampling distributions were: DT_L = [3.0, 11.0], T_O = [28.0, 36.0], DT_U = [36.1, 42.0]. The sensitivity analysis of the procedure for calculation of effective temperature was

tested on the interval of air temperature [0, 44.0]. The sensitivity analysis was performed with 3,000 bootstrap replicates.

2.6. Model calibration

2.6.1. Lower development threshold

The lower temperature threshold for the movement of *P. chalcographus* was found to be 8°C (Zumr, 1982). Usually, each developmental stage has its own lower developmental threshold (Wermelinger and Seifert, 1998). PHENIPS and RITY-2 use average DT_L from egg to pupae (Baier *et al.*, 2007; Ogris *et al.*, 2019). Therefore, we assumed the possibility that the DT_L for development from egg to adult of *P. chalcographus* could be different than the DT_L for the movement of adult beetles (8°C).

The most appropriate DT_L was chosen with an iteration procedure where the lowest mean absolute error (MAE) of predicted emergence of filial beetles from trap logs was observed. DT_L was sought in the range from 3.0 to 11.0°C at 0.1°C increments.

2.6.2. Spring swarming, onset of infestation and end of mass swarming

To predict the onset of spring swarming and infestation, we compared the observed onset of trap catches and trap log infestation with the observed thermal conditions for flight activity. Additionally, the observed onset of spring swarming and host tree colonization by *P. chalcographus* was compared with the cumulative thermal sum of maximum air temperatures above DT_L accumulated from the latest date onwards using estimated temperature data.

According to Slovenian records, the onset of spring swarming and host tree colonization can already occur in the beginning of March (Jurc, 2008; Ogris, 2012). Therefore, accumulation of the thermal sum must begin before that. We used an iterative procedure to identify the latest date to start calculation of the cumulative thermal sum for the onset of spring swarming and host tree colonization (Ogris *et al.*, 2019). We chose the date that produced the lowest MAE of the predicted onset of spring swarming and host tree colonization.

We calibrated end of mass swarming in late summer with an independent dataset of 1,017 flight-barrier Theysohn® traps monitored by Slovenia Forest Service in the period from 2015 to 2019 at least at 11-day intervals (GIS and ZGS, 2020; Ogris, 2012, 2020). 95.4% of traps were equipped with a pheromone product PC ECOLURE (Fytofarm Ltd., Bratislava, Slovak Republic) while the rest had Chalcoprax® (BASF SE, Ludwigshafen, Germany). Because the traps were monitored at different intervals and different dates, the data was harmonized and averaged to ten- to eleven-day periods from the beginning of April to the end of October.

2.6.3. Brood development

In order to describe the relation between the developmental rate of *P. chalcographus* and temperature, we used both a linear function with only DT_L (see equation A.7) and a nonlinear function as proposed by Wermelinger and Seifert (1998) for *I. typographus* and calibrated for *P. chalcographus*.

Effective temperatures for development from the egg stage to the emergence of mature filial beetles were adapted using T_O, DT_L and DT_U. T_O and DT_U were not known for *P. chalcographus* at the time of the study. DT_U was set with the help of a database of thermal requirements for insects and mites (Jarošík *et al.*, 2011, 2012). The DT_U for species of the Curculionidae family is 39.4°C. This DT_U was used by CHAPY. To our knowledge, T_O for *P. chalcographus* has not yet been studied. We assumed that T_O is similar to *I. typographus* (Wermelinger and Seifert, 1998) and *I. duplicatus* (Davídková and Doležal, 2019). Therefore, we considered 30.0°C as T_O.

The effective temperature (T_{eff}) was estimated using the nonlinear function of the modified Logan model (Lactin *et al.*, 1995; Logan *et al.*, 1976), with the assumption that the relative developmental rate increases linearly within the range of DT_L and T_O and that the relative developmental rate is equal to 1 at T_O. For temperatures outside the lower and upper temperature thresholds ($T \leq DT_L$ and

$T \geq DT_U$), T_{eff} was set to zero. The effective temperature within the range between To and DT_U was calculated with the nonlinear function of the modified Logan model whose parameters were estimated iteratively by means of nonlinear regression analysis within the range of DT_L and DT_U.

A thermal sum of 518–598 dd is required for the total development of *P. chalcographus* (Harding *et al.*, 1986). The upper limit of this range was used as a reference value for comparison (K = 598 dd). Relative thermal sums for the egg, larval, pupal and maturation feeding stages are not known for *P. chalcographus*. Therefore, we assumed that the relative proportions are similar to *I. typographus* (Wermelinger and Seifert, 1998): egg 10%, larvae 40%, pupae 10% and maturation feeding 40%, respectively.

A study performed by Harding *et al.* (1986) recorded re-emergence; therefore, formation of sister broods is also included in the calculation of the phenology model. Sister broods or re-emergence is a phenomenon common to the spruce bark beetle and several other species of the Scolytinae subfamily (Davídková and Doležal, 2017). After mating, the female deposits the first brood. It may then re-emerge and, after regeneration feeding, re-enter the same or a different tree to produce one or more so-called sister broods (Anderbrant and Löfqvist, 1988; Wermelinger and Seifert, 1999).

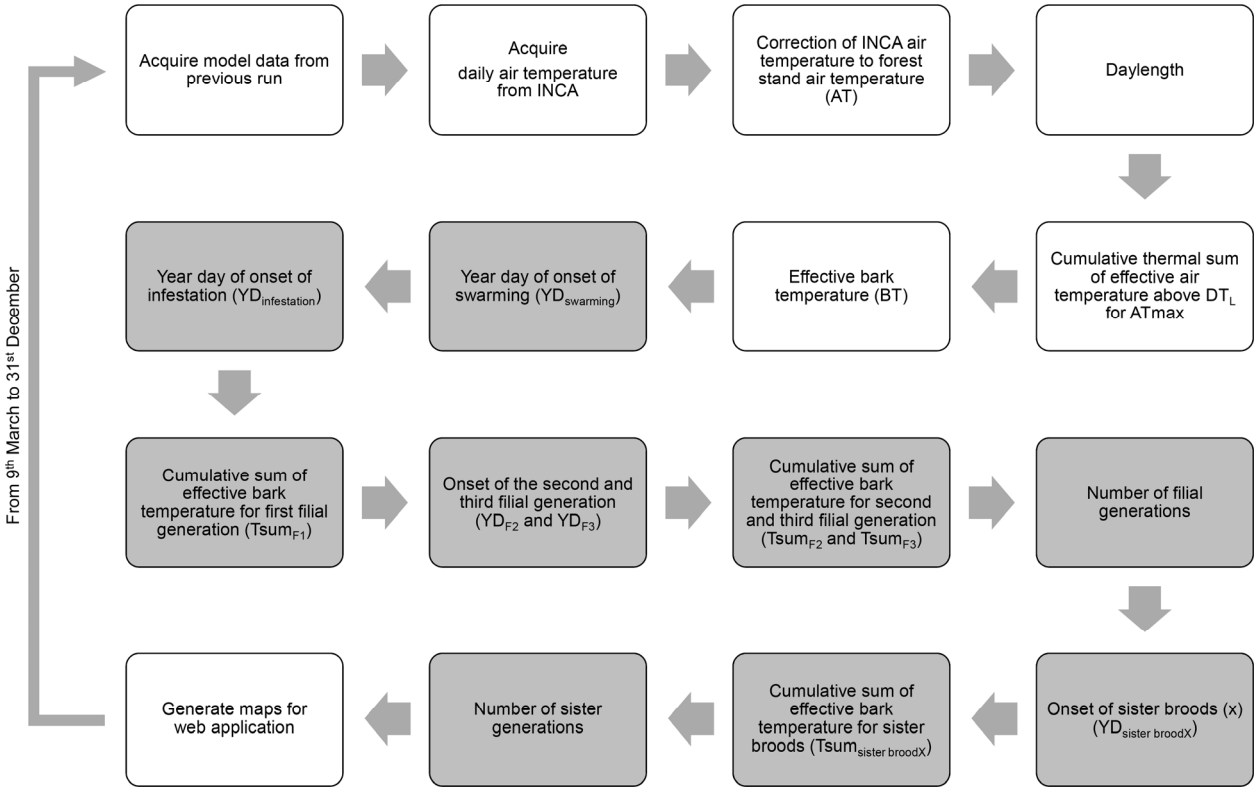

Fig. 1. Diagram of the CHAPY model. The model is calculated stepwise and every day from 9th March to 31st December. White boxes are preliminary steps and grey boxes depict core computation steps. A detailed description of the model computation is given in Appendix A.

A conceptual diagram summarizing the main steps of the CHAPY model calculation is presented in Fig. 1. A detailed description of the model computation along with the formulae is given in Appendix A.

2.7. Model validation

To determine the accuracy of the phenological model, we compared the effective thermal sum (computed with Eqs. (A.7)–(A.9) using 30-min recorded bark temperatures) at the date of imago emergence with K. For validation of the predicted onset of emergence of filial beetles calculated from the INCA data, we compared the estimated effective thermal sum at the date of emergence predicted by the model with K.

The development rate was calculated with the MIN, AVG and MAX scenarios according to the BTmin, BTavg and BTmax effective bark temperatures, respectively (Eqs. (A.4)–(A.9)). The onset of swarming and infestation was always calculated using corrected daily maximum air temperatures from the INCA (ATmax; Eqs. (A.10) and (A.11)).

Onset of swarming was additionally validated with independent dataset of 22 flight-barrier Theysohn® traps equipped with a pheromone product PC ECOLURE TUBUS (Fytofarm Ltd., Bratislava, Slovak Republic). Those pheromone traps were monitored by Slovenia Forest Service during 2015–2020 at least once per week. Similarly, onset of infestation was additionally validated with independent dataset of 78 trap trees that were monitored at least once per week by Slovenia Forest Service (GIS and ZGS, 2020; Ogris, 2012, 2020).

2.8. Statistics and data management

Statistical analyses were performed using the R software environment for statistical computing (R Core Team, 2018), wherein the following packages were used: sensitivity (Iooss *et al.*, 2019), RODBC (Ripley and Lapsley, 2017), DescTools (Signorell, 2018) and raster (Hijmans, 2016). Linear relations were analysed using linear regression analysis. For nonlinear relations, the nls (Nonlinear Least Squares) procedure was used. A one-sample Kolmogorov-Smirnov test was applied to verify normal distribution of test variables. Pairs of means were compared using the paired sample *t*-test. Deviations of the mean of a single variable from a specified test value were tested by the one-sample *t*-test. We used Microsoft SQL Server 2016 as a database for modelling and calculation of thermal sums for predicting phenological events. Graphs were drawn with Microsoft Excel for Office 365 (16.0).

3. Results

3.1. Sensitivity analysis of the effective temperature

The first order (main) effect explained in total 8.0% of the output variation, where DT_L had the highest and DT_U the lowest effect (Fig. 2). The rest of the variation was explained by air temperature. The second-order interaction (total) effect explained in total 30.4% of the variation of the parameters on the predictions of the effective temperature, where DT_L explained nearly the same level of variance as the first order effect, DT_U had an even smaller influence on the output variation, and T_O had the greatest interaction effect among the parameters and a substantial increase in comparison to the first order effect.

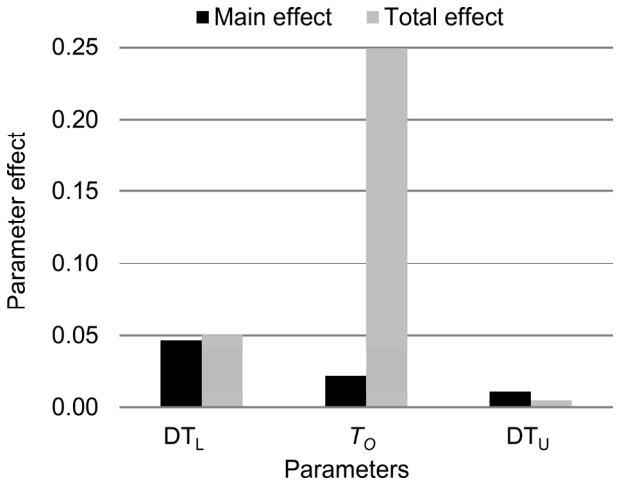

Fig. 2. Main and total effects of the parameters on the predictions of the effective temperature. The main effect (or first order effect) quantifies the individual effect of a parameter, i.e. without interactions. The total effect represents the first and second order effects, i.e. with second-order interaction effects. These effects quantify the proportion of variance of the model's prediction explained by the variation of a given parameter.

3.2. Model calibration

3.2.1. Lower development threshold

The procedure for calculation of effective temperature includes three parameters: DT_L, To and DT_U. The observed temperatures in the field and the growth chambers were not greater than To. Thus, calibration of To and DT_U was not possible due to lack of data. Therefore, only DT_L was calibrated, while To and DT_U were assumed as already explained in the Methods section.

The most appropriate DT_L was chosen with the iteration procedure where the lowest MAE of the predicted emergence of filial beetles from trap logs was observed. Low MAEs below 2.28 days were achieved in the range between 6.1 and 8.3°C. The lowest MAE with the lowest standard error was achieved at 7.4°C, which was chosen as the DT_L (Fig. 3). A steep increase in MAE was observed above 8.3°C and below 4.5°C.

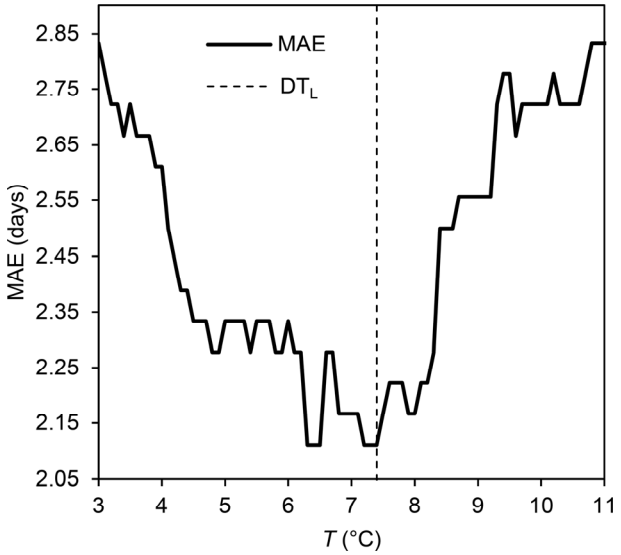

Fig. 3. Mean absolute error (MAE) of predicted emergence of filial beetles from trap logs according to the variable lower developmental threshold (DT_L) (vertical dotted line indicates chosen DT_L at a temperature of 7.4°C)

3.2.2. Effective temperature above optimum temperature

The effective temperature within the range between To and DT_U was calculated with Eq. (5). The parameters α, β, γ and T_{max} were estimated iteratively by means of nonlinear regression analysis within the range of DT_L and DT_U (Fig. 4).

$$T_{eff} = (To - DT_L) \times (\exp(\alpha \times T) - \exp(\alpha \times T_{max} - (T_{max} - T)/\beta) - \gamma) \quad (5)$$

where $\alpha = 0.031$; $\beta = 5.3$; $\gamma = 1.25$; $T_{max} = 41.97$; $T_{eff} = 0$ when $T \leq DT_L$ and $T \geq DT_U$

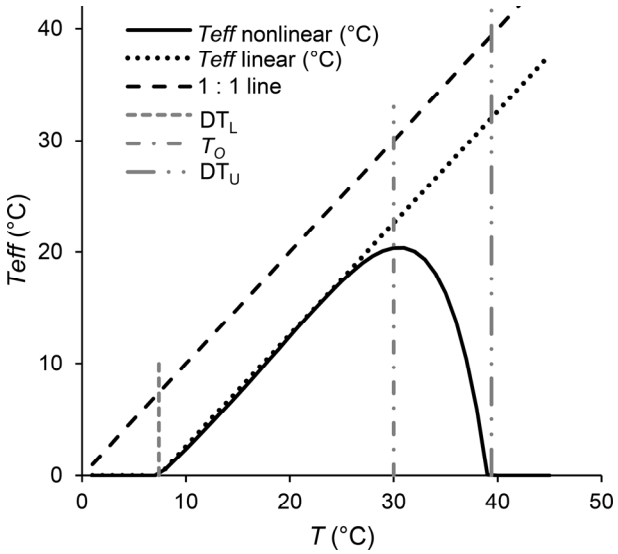

Fig. 4. Relationship between naturally occurring temperatures (*T*) and effective temperatures for the development of *P. chalcographus* (*Teff* nonlinear: effective temperature according to Eq. (5); *Teff* linear: effective temperature of the linear model using only the lower threshold)

3.2.3. Spring date threshold of the model calculation

Factors other than the lower air temperature threshold for flight activity (ATmax > 16.8°C; Lobinger, 1994; Zumr, 1982) might influence the start of reproductive activities in the spring. We assumed that the thermal sum determines the onset of swarming and infestation. The earliest onset of swarming occurred at the Brode and Kamnik locations on 20/03/2017. Therefore, the accumulation of thermal sum had to start before that date. The lowest mean absolute error for prediction of the onset of swarming and infestation was determined with an iterative procedure (Ogris *et al.*, 2019). The latest, lowest MAE was achieved on 9th March (Fig. 5), which was chosen as the spring date threshold of the model calculation.

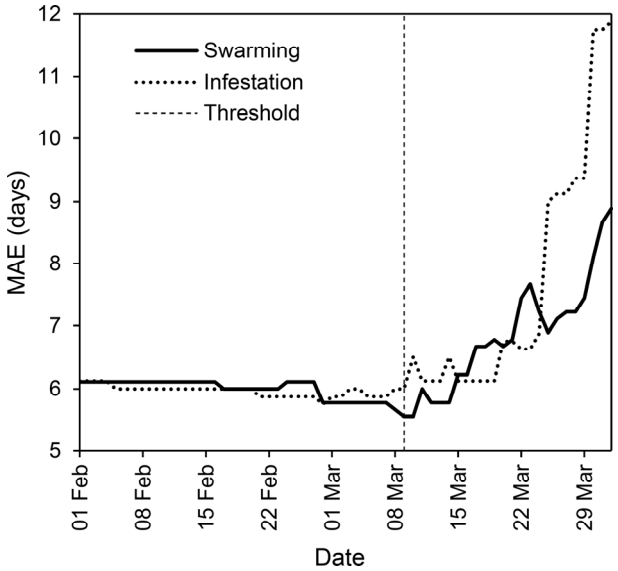

Fig. 5. Date threshold for calculation of the onset of spring swarming and host tree infestation (vertical dotted line indicates a date threshold of 9th March)

3.2.4. End of mass swarming

Mean number of beetles caught in the pheromone traps gradually decreased from middle of July to the beginning of September (Fig. 6). A linear relationship between the mean daylength and the mean number of caught beetles per ten- to eleven-day periods from the middle of July to the beginning of September was found with very high correlation coefficient (R = 0.986) (Fig. 7). In September, at daylength below 13.6 h, a very low number of beetles were caught (on average 807)

in the traps even though ATmax was sufficiently high for swarming (22.1–26.4°C) (Fig. 6). In October, no swarming was recorded because ATmax was below the flight temperature (< 15.6°C). We concluded that swarming of *P. chalcographus* beetles in the late summer was mainly limited by daylength while maximum air temperature had only a minor effect at daylength below 13.6 h. Finally, we included daylength limit of 13.6 h into the model as a threshold for end of swarming in the late summer. Additionally, the same pattern was found in the spring, i.e. mass swarming started when the mean daylength was greater than 13.5 h (Fig. 6).

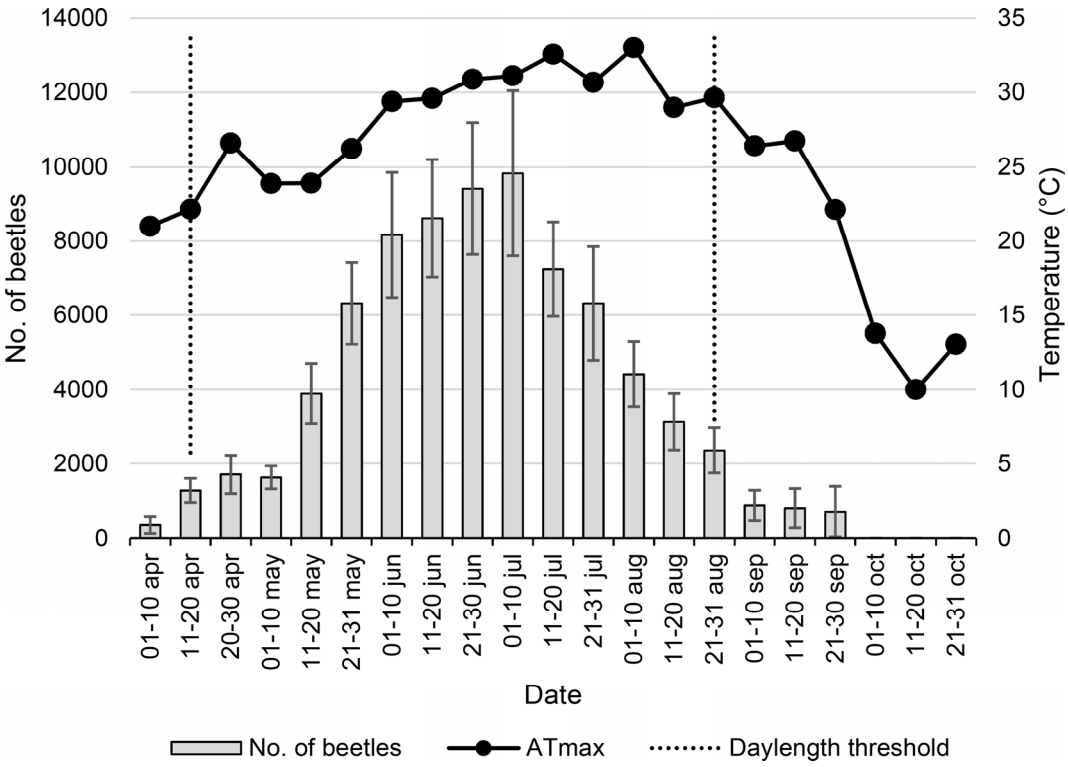

Fig. 6. Mean number of beetles caught in pheromone traps and mean maximum air temperature (ATmax) from April to October in the period from 2015 to 2019 per ten- to eleven-day periods (N = 1,017). Error bars show 95% confidence interval of mean number of beetles per period. Two vertical dotted lines depicts daylength threshold for mass swarming in the spring and the late summer, both at 13.6 h.

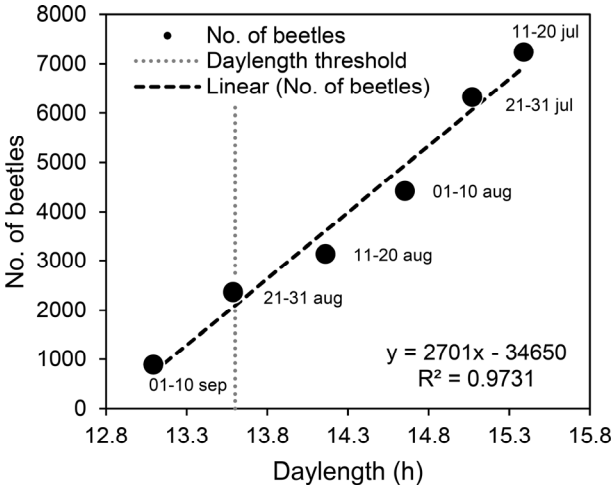

Fig. 7. Linear regression between mean daylength and mean number of beetles caught from 11th July to 10th September per ten- to eleven-day periods. Vertical dotted line shows selected daylength threshold at 13.6 h for mass swarming in late summer.

3.3. Model validation

3.3.1. Daily effective thermal sum

The estimated daily effective thermal sum showed a MAE of 1.01 dd and a root mean square error (RMSE) of 1.34 dd for mean bark temperature. The correlation between the estimated and observed daily thermal sums was relatively high for mean bark temperature, with $R^2 = 0.86$, and was significant ($P < 0.001$).

The modelled cumulative effective thermal sum for the whole study period showed a MAE of 72.6 dd and a RMSE of 80.3 dd for mean bark temperature (Table 2). An average observed BTeff was 5.7 dd per day; therefore, MAE of 72.6 dd resulted in an average error of 12.8 days during an average study period of 91.6 days. The variability explained between the estimated and observed cumulative thermal sums was low ($R^2 = 0.086$) and not significant ($P = 0.244$).

Table 2. Observed and estimated cumulative effective thermal sum for mean bark temperature (BTeff) for the whole study period in the field, and deviation of estimated from observed data (MAE: mean absolute error)

Location of trap log	Start *	End *	Observed BTeff (dd)	Predicted BTeff (dd)	Deviation (dd)
Vodice	15/03/2017	19/06/2017	504.3	442.4	–61.9
Kamnik	15/03/2017	12/06/2017	433.3	373.7	–59.5
Brode	15/03/2017	26/06/2017	439.3	526.7	87.4
Prevala	15/03/2017	10/07/2017	579.3	674.6	95.4
Medvedica	22/03/2018	26/06/2018	587.1	480.1	–107.0
Turjak	22/03/2018	26/06/2018	505.0	480.1	–24.9
Erjavčev laz	19/04/2018	26/06/2018	568.7	446.6	–122.1
Mokrc	19/04/2018	26/06/2018	424.0	446.6	22.6
				Minimum	–122.1
				Maximum	95.4
				MAE	72.6 [b]

* Study period for measuring effective bark temperatures in the field. Note: This period is different from the period for evaluation of brood development.

Mean cumulative observed and estimated thermal sums of mean bark temperature did not differ significantly ($t = –0.726$; $P = 0.4913$). Estimated cumulative thermal sums were underestimated by –21.2 dd for mean bark temperature. The confidence interval for the ratio between the estimated and observed thermal sums was 96.4 ± 13.2%.

3.3.2. Spring swarming and onset of infestation

Bark beetles were captured in pheromone traps when the daily mean maximum air temperature (ATmax) exceeded 17.3°C. Our observations indicate that *P. chalcographus* initiated flight activity at a daily minimum observed ATmax of 13.0°C, which corresponds to the estimated daily maximum air temperature of 15.6°C. The latter was used as the threshold for the phenological model calculation (see Appendix A).

Major flight (the first day with a catch > 100 individuals than that of the last counting) occurred on days when ATmax was above 20.9°C. The first attacks of *P. chalcographus* on trap logs in spring were observed at a mean ATmax of 21.3 ± 2.3°C. Initial infestation of trap trees occurred 6–40 days after the initial swarming (Table 3). The longest gap of 40 days between the onset of swarming and onset of infestation occurred at the highest location (Prevala). Locations with a lower elevation had a lower delay of initial infestation after the onset of swarming, i.e. 6–23 days (Table 1 and Table 3).

Our observations indicate that flight activity was initiated when the thermal sum (ATmax > 7.4°C) accumulated from 9th March onwards was on average 80.5 ± 26.2 dd. The first colonization of trap logs was observed when the thermal sum reached 216.5 ± 52.0 dd (Table 3). A variance of these results expressed through confidence interval can be partially explained with an interval of monitoring which was a source of uncertainty. Two- to three-day intervals with an average *Teff* = 3.6 dd represented an uncertainty up to 10.9 dd, while seven-day intervals with an average *Teff* = 5.6 dd represented an uncertainty up to 39.2 dd (Fig. 8).

Table 3. Recorded onset of spring swarming, onset of infestation of trap logs, estimated onset of swarming and infestation, and deviation of estimated onset from observed data (MAE: mean absolute error of estimated onset of swarming and infestation)

Location of trap/trap log	Observed onset [d]		Thermal sum (dd)		Estimated onset		Deviation (days)	
	Swarming [a]	Infestation [b]	Swarming	Infestation	Swarming	Infestation	Swarming	Infestation
Vodice	24/03/2017	03/04/2017	106.5	212.2	21/03/2017	03/04/2017	3	0
Kamnik	20/03/2017	03/04/2017	62.4	197.9	24/03/2017	09/04/2017	–4	–6
Brode	20/03/2017	03/04/2017	37.7	134.6	24/03/2017	10/04/2017	–4	–7
Prevala	12/04/2017	22/05/2017	139.4	293.8	29/03/2017	12/05/2017	14	10
Medvedica	02/04/2018	25/04/2018	61.9	305.5	08/04/2018	21/04/2018	–6	4
Turjak	13/04/2018	25/04/2018	106.1	245.8	08/04/2018	22/04/2018	5	3
Erjavčev laz	08/04/2018	25/04/2018	38.0	195.2	19/04/2018	02/05/2018	–11	–7
Mokrc	19/04/2018	25/04/2018	77.8	146.9	19/04/2018	06/05/2018	0	–11
Vorenčkojca [c]	17/04/2018		94.7		14/04/2018	25/04/2018	3	
						Minimum	–11	–11
	Mean thermal sum		80.5	216.5		Maximum	14	10
	Confidence interval (95%)		26.2	52.0		MAE	5.6	6.0

[a] Onset of swarming was observed at two- to three-day intervals. The date in the table indicates the date of monitoring.

[b] Onset of infestation was observed every seven days. The date in the table indicates the date of monitoring.

[c] At the Vorenčkojca location, only the onset of swarming was monitored in the pheromone trap.

[d] The earliest onset of swarming and infestation.

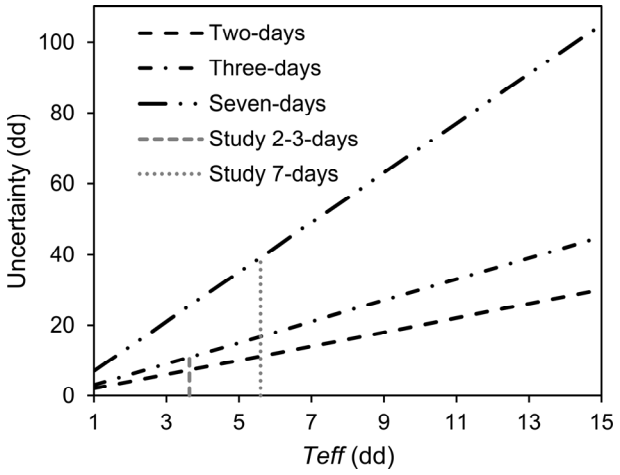

Fig. 8. Uncertainty of effective temperature according to different intervals of monitoring. First dashed vertical line at an average *Teff* = 3.6 dd represented an uncertainty of two- to three-day intervals of monitoring relevant to this study. Second dotted vertical line at an average *Teff* = 5.6 dd represented an uncertainty of seven-day intervals.

Using the accumulated thermal sum in combination with flight activity and date threshold, the onset of spring swarming was estimated with a MAE of 5.6 days, and the onset of trap log colonization in spring was estimated with a MAE of 6.0 days (Table 3). Furthermore, both onset of spring swarming and onset of infestation were estimated with a similar MAE of 5.8 days with the independent dataset of 22 pheromone traps and 78 trap trees. The difference between the observed and predicted onset of swarming of nine pheromone traps was 11 days earlier at minimum and 14 days later at maximum. The difference between the observed and predicted onset of infestation of eight trap logs was 11 days earlier at minimum and 10 days later at maximum (Table 3).

3.3.3. Brood development

All eight trap logs felled in 2017 and 2018 were colonized by *P. chalcographus* (Table 3). Eight trap logs were monitored until the emergence of filial beetles, and altogether 18 sample chunks were monitored in growth chambers at two constant temperatures (23°C and 28°C) every day with different onsets of infestation (Table S1).

For validation of the brood development rate, we compared the observed onset of emergence of filial beetles with the thermal sum of 30-min measured bark temperatures at four positions around the trunk (Eqs. (A.7)–(A.9)) using the same calculation procedure of Harding *et al.* (1986) including different DT_L = 8.0°C provided by Zumr (1982). For comparison, we used the reference value K = 598 dd provided by Harding *et al.* (1986) which used different DT_L = 8°C from ours DT_L = 7.4°C. To make this comparison, we had to use the same calculation procedure along the same DT_L = 8°C. The thermal sum at the time of emergence was not significantly different from the test value (K = 598 dd) for both observed emergence and predicted emergence from hourly and daily data (P > 0.05, Table 4). The mean deviations of the calculated thermal sum from the required thermal sum (598 dd) ranged from 15.3 to 25.3 dd for hourly data and 6.9 to 11.1 dd for daily data (Table 4). Therefore, daily air temperature was used to calculate the phenological model.

Table 4. Mean value, standard deviation (S.D.), test statistics (one-sample t-test with test value K = 598 dd), relative mean error (RPME) and mean difference from K (ME) of the thermal sum at the date of observed and predicted emergence of filial beetles from trap logs according to hourly and daily data (d.f. = 17). Thermal sums were calculated with the procedure of Harding *et al.* (1986) including different DT_L = 8.0°C provided by Zumr (1982).

Emergence	Mean value (dd)	S.D. (dd)	t-Value	P	RPME (%)	ME (dd)
Observed from 30-min data	582.7	51.5	–1.2566	0.226	2.55	15.3
Predicted from hourly data	572.7	52.8	–2.0301	0.058	4.23	25.3
Observed from daily data	609.1	44.1	1.0665	0.301	1.85	11.1
Predicted from daily data	591.1	60.7	–0.4816	0.636	1.15	6.9

Following the CHAPY calculation procedure (Appendix A), the observed mean thermal sum for the total development of filial beetles was 652.8 ± 22.7°C (Table S1). The predicted mean thermal sum for the total development of filial beetles was 635.4 ± 31.4°C. The observed mean thermal sum was not significantly different from the predicted mean thermal sum for the total development of filial beetles (t = 1.1881, d.f. = 17, P = 0.251). The implementation of the CHAPY model uses the INCA dataset as model input; thus, the predicted thermal sum of 635.4 dd was used as the thermal sum required for total development from egg to mature beetle (model parameter K; see Appendix A). The predicted emergence of filial beetles was estimated with a MAE of 2.11 days with a minimum of nine days too early and four days too late. The deviation of the estimated emergence from the observed data had high correlation with the estimated thermal sum and was significant (R^2 = 0.985, P < 0.001).

The duration of three developmental stages was observed, i.e. egg, larval and a combination of the pupal and teneral adult stages. The relative durations of the developmental stages of *P. chalcographus* were calculated with regard to K. The mean duration of the egg, larval and combination of the pupal and teneral adult developmental stages was 9.4%, 58.2% and 32.4%, respectively (Table 5)**Error! Reference source not found.**. In accordance with the reference values (Wermelinger and Seifert, 1998), the mean difference for the duration of the egg stage was 0.6% shorter, the larval stage was 18.2% longer and the combination of the pupal-teneral adult stage was 17.6% shorter (Table 5**Error! Reference source not found.**). The duration of developmental stages in the phenology model was calculated with adjusted mean values: egg 10%, larvae 60%, pupae 10%, teneral adult (maturation feeding) 20% (see Appendix A).

Table 5: Relative durations of developmental stages of *P. chalcographus* with regard to the thermal sum required for total development (K = 635.4 dd) and mean error in accordance with reference values* (N = 8)

Developmental stage	Duration (%)			ME (%)*
	Mean	Min	Max	
Egg	9.4	5.2	13.5	–0.6
Larvae	58.2	46.1	74.0	18.2
Pupae + teneral adult	32.4	18.9	46.3	–17.6

* Mean error according to reference values for egg 10%, larvae 40%, pupae + teneral adult 50% in *I. typographus* according to Wermelinger and Seifert (1998).

3.3.4. Re-emergence

The earliest time of re-emergence of parental beetles was observed 43 days after trap log colonization at the Prevala location. The relative thermal sum at the time of re-emergence of parental beetles was on average 69.2 ± 4.8% with a minimum of 56.1% calculated from daily observed bark temperatures (Table S1). The relative thermal sum (expressed as a percentage of the thermal sum required for total development) at the time of re-emergence was on average 68.0 ± 4.6% with a minimum of 52.7% according to the estimated bark temperature. These results are based on the daily observations in the two plant growth chambers. The minimum observed time of re-emergence of parental beetles is more likely correct than the average value. Thus, for modelling the re-emergence of parental beetles, we used a relative thermal sum of 50%, i.e. 317.7 dd, which is an approximation of the observed minimum (see Eq. (A.13)).

4. Discussion

We validated several aspects of CHAPY: the modelled and actual timing of spring swarming, onset of infestation, re-emergence of parental beetles, completion of the first filial generation and the duration of developmental stages. We found remarkable agreement between the daily effective thermal sums of modelled and measured mean bark temperatures (Ogris *et al.*, 2019). Thus, air temperature data from the INCA were able to quite accurately predict effective thermal sum. Cumulative thermal sums were generally slightly underestimated. Using accumulated thermal sum in combination with flight activity and date threshold, the onset of spring swarming and infestation was estimated with a relatively low mean absolute error. Re-emergence of parental beetles was observed at approximately half of the relative thermal sum required for total development. The thermal sum at the time of emergence was not significantly different from the reference value for both observed and predicted emergence from hourly and daily data. The estimated and observed developmental rates were not always comparable between observations and predictions, especially for higher elevations. Therefore, CHAPY was calculated according to the three scenarios to encompass all possible outcomes (Eqs. (A.1)–(A.6)).

In this study, we used the RITY-2 model (Ogris *et al.*, 2019), which is based on the PHENIPS model (Baier *et al.*, 2007), as the framework for modelling *P. chalcographus*, and the CHAPY model was the result. RITY-2 was substantially changed to reflect the phenology of *P. chalcographus*: (1) The effective bark temperature between T_O and DT_U was calculated with new sets of parameters for the non-linear function (Eq. (5); (A.8)); (2) The date threshold for spring swarming was found with an iterative procedure to be 9th March; (3) The limiting ATmax for the onset of swarming was set to 15.6°C; (4) The onset of swarming was calculated with a thermal sum of 80.5 dd (Eq. (A.10)); (5) The onset of infestation was calculated with a thermal sum of 216.5 dd (Eq. (A.11)); (6) The necessary thermal sum for total development (K) was set to 635.4 dd (Eq. (A.12)); and (7) Preimaginal development was set at a relative thermal sum of 80% of the thermal sum required for total development.

During the CHAPY validation process, several knowledge gaps in the phenology of *P. chalcographus* were identified. Therefore, several assumptions were made for key elements in the biology of the six-toothed spruce bark beetle: (1) T_O was assumed to be 30.0°C; (2) DT_U was

assumed to be 39.4°C; (3) DT_L for each developmental stage is missing; however, in our study it was found that a DT_L of 7.4°C had the lowest MAE of predicted emergence of filial beetles and it was assumed that 7.4°C represents a mean DT_L for development of *P. chalcographus* from egg to mature beetle; (4) The date threshold for calculation of the onset of swarming was searched with an iterative procedure and it was assumed to be 9th March; (5) The daylength limit for the onset of a new filial or sister brood was assumed to be at 13.6 h on the basis of monitoring of 1,017 pheromone traps (Eqs. (A.13)–(A.15)). The daylength threshold was assumed solely on the swarming data without verifying if diapause actually initiated. Furthermore, diapause initiation is implemented in a very strict manner where only daylength (≥ 13.6 h) is considered even though it probably could also be influenced by temperature (Führer and Chen, 1979). However, according to our study swarming is substantially dropped after the daylength < 13.6 h even though the temperatures were favourable for flight activity; (6) The model calculation continues into a winter and it is concluded by 31st December as brood development might continue during winter at temperatures above DT_L (Štefková *et al.*, 2017). However, winter mortality might be slightly underestimated, and number of generations slightly overestimated in the case of an early frost period e.g. in November and later in December; (7) Since solid data on the thermal sum of effective bark temperatures for each developmental stage is missing, duration thresholds for each developmental stage were set according to our recorded data; (8) Since the adult stage is the most widespread overwintering stage (Koštál *et al.*, 2014), it is assumed that preimaginal stages of *P. chalcographus* do not survive winter. All these assumptions could have a substantial impact on CHAPY output. Each of these assumptions represents an ideal opportunity for further research on the phenology of *P. chalcographus* and the further improvement of CHAPY. The first priority would be finding an observed optimum temperature which had the greatest total effect in the sensitivity analysis among the parameters for the predictions of the effective temperatures (Fig. 2). The next priority would be finding actual relationship between daylength limit and temperature for the diapause initiation as this might have considerable effect on part of model outputs, e.g. number of generations.

Daily and cumulative estimated thermal sums fitted less well for CHAPY than for RITY-2, supposedly due to the assumed optimum temperature, for which the total effect was high according to the sensitivity analysis. The estimated cumulative thermal sum of effective bark temperatures was underestimated by 3.6% (CHAPY) and 2.5% (RITY-2). Therefore, the observed development rate was usually slightly faster than modelled. The validation for the study sites at lower elevations showed quite good agreement between predicted and observed cumulative thermal sums while the higher locations had greater error of predicted cumulative thermal sum. This pattern was supported by the high correlation that was found between the deviation of estimated emergence from observed data and estimated thermal sum. This rule could indicate that locations at higher elevations might need a higher cumulative thermal sum for the total development of filial beetles. Nevertheless, further research is needed to prove this hypothesis.

In this study, we observed the re-emergence of parental beetles that established a sister brood. In contrast, Lekander and Lindelöw (1977) found no indication of a sister brood in Sweden, and according to histological examinations by Zumr and Soldan (1981), *P. chalcographus* has only one reproductive cycle and dies after oviposition. However, there is increasing evidence that at least one sister brood does occur in Central European *P. chalcographus* populations according to our observations (see Table S1) and several other studies (Harding *et al.*, 1986; Kacprzyk and Bednarz, 2015; Kasumović, 2016). These contradictory observations about the existence of a sister brood demand further research to clarify this phenomenon in *P. chalcographus*. We assume that geographic latitude, daylength, temperature variation and genetic differences between populations of *P. chalcographus* might play a considerable role.

Furthermore, our study had a small sample consisting of nine pheromone traps and only eight trap logs felled at different locations with different elevations, aspects and slopes (Table 1). We were therefore not able to fully capture the overall variability of the spatiotemporal dynamics of *P.*

chalcographus in Slovenia. We believe that a larger sample encompassing all biogeographical regions in Slovenia equally would give somewhat different thresholds and parameters of CHAPY following the same calibration procedures. CHAPY can be used at any location; however, regional-specific thresholds need to be calibrated and validated to reflect the specific conditions of the region.

CHAPY was implemented into two public web applications (in Slovenian only). The first is point-based and produces a chart of relative thermal sums of the predicted development of *P. chalcographus* according to the MIN, AVG and MAX scenarios for any location in Slovenia (Ogris, 2019c). The second web application is raster-based and produces several maps of the predicted development of *P. chalcographus* for the whole Slovenia (Ogris, 2019d). On the map we can observe time series for the development of bark beetle developmental stages for several filial and sister broods, onset of spring swarming, onset of infestation of different broods, and number of filial and sister broods. The source codes for both applications are publicly available (Ogris, 2019a, b).

Potential applications of CHAPY for monitoring and management of *P. chalcographus* are numerous. In our case, CHAPY is used along with RITY-2 to improve the efficiency of bark beetle monitoring; it is incorporated into an automatic e-messaging system that informs 14 regional and 69 local units of the Slovenia Forest Service about the predicted onset of swarming and completion of first filial generation (Ogris *et al.*, 2019), i.e. the key dates for evaluation of the *P. chalcographus* population abundance at the trap location. When the catch in the trap from the beginning of spring swarming until the end of the first generation exceeds 20,000 beetles, an outbreak is imminent and an attack on healthy host trees can be expected (RS, 2009). Once the risk-threshold has been exceeded, several control strategies can be applied, i.e. increasing the number of the traps (mass-trapping), setting-up trap trees, conducting a more careful survey of spruce forests, and eventually cutting recently attacked trees via sanitation programmes (Faccoli and Stergulc, 2004, 2006; Jurc *et al.*, 2017; Schroeder, 2013). All these actions are carried out to keep *P. chalcographus* populations at endemic levels, thus avoiding outbreaks and subsequent damage that could be caused by *I. typographus*. Furthermore, the utilization of detailed data on air temperature for modelling bark temperatures provides a precise monitoring of the actual state of bark beetle development at the specific model grid cell. CHAPY simulates the maximum number of generations at each model grid cell, what can be used for assessing the likelihood of outbreaks and their potential impacts at the regional scale. The last but not the least, the model can be used for long term assessment of the climate change effects while modelling the change in maximum number of generations at different temperature scenarios.

5. Conclusions

The CHAPY model includes the prediction of the time of spring swarming, onset of infestation, re-emergence of parental beetles, and the number and emergence time of filial and sister broods. As several model parameters were missing, a sensitivity analysis was performed, and model parameters were calibrated to best fit the observed data. To validate the model, we compared the recorded air temperature, bark temperature, flight activity and developmental progress in trap logs at various altitudes and relief aspects with phenological events predicted by the model. Additionally, independent datasets of pheromone traps and trap logs were used to validate onset of spring swarming, onset of infestation, and end of mass swarming in late summer. The result is a validated, calibrated and implemented CHAPY model.

The sensitivity analysis, validation and calibration procedure of CHAPY showed that the phenological model quite accurately simulates the seasonal dynamics of *P. chalcographus* populations. The model was successfully incorporated into publicly available web tools. To our knowledge, CHAPY is the first comprehensive phenological model for *P. chalcographus* and thus contributes to progress in ecological modelling. Nevertheless, CHAPY is based on several assumptions that provide opportunities for further phenology research on the second most damaging spruce bark beetle in Central Europe and thus further improvement of the model.

Acknowledgements
We thank Danijel Borković (Biotechnical Faculty), who carried out most of the field work by monitoring the trap logs; Boštjan Zupanc (Slovenian Forestry Institute, SFI) for managing the meteorological stations; Marija Kolšek (Slovenia Forest Service, SFS) for organising trap settings; Miha Zabret (SFS), Jože Kozjek (SFS), Anže Mihelič (SFS), Milan Podlogar (SFS), Matej Zamernik (SFS), Jože Oberstar (SFS), Tomaž Černe (SFS), Branko Krulič (SFS), Pavle Košir (SFS), Matjaž Pajnič (SFS) and Robert Krajnc (SFI) for field work; Špela Jagodic (SFI) for help in the laboratory; Lucija Odar (SFS) for monitoring the pheromone trap at the Vorenčkojca location; Neva Pristov (Slovenian Environment Agency) for providing INCA and ALADIN data; and forest owners for their permission to perform the study in their forests. We thank Philip Jan Nagel for language editing. We are especially grateful to the anonymous reviewer for constructive comments which improved the manuscript greatly.

Funding: This work was supported by the Ministry of Agriculture, Forestry and Food and the Slovenian Research Agency (V4-1623, P4-0107).

Declaration of interests

The authors declare that they have no known competing financial interests or personal relationships that could have appeared to influence the work reported in this paper.

Appendix A

A.1. Air temperature, bark temperature and effective bark temperature

Minimum, mean and maximum daily air temperatures (AT) in the stand were calculated using the linear models and daily air temperature from the INCA system (I_{min}, I_{mean}, I_{max}) for each location x and day i (x_i) (Ogris *et al.*, 2019):

$$ATmin(x_i) = 1.44 + 0.82 \times I_{min}(x_i) \quad (A.1)$$

$$ATmean(x_i) = 0.50 + 0.81 \times I_{mean}(x_i) \quad (A.2)$$

$$ATmax(x_i) = 1.03 + 0.86 \times I_{max}(x_i) \quad (A.3)$$

Minimum, mean and maximum bark temperatures (BT) were calculated using linear models and daily estimated air temperatures (Ogris *et al.*, 2019):

$$BTmin(x_i) = 0.56 + 0.99 \times ATmin(x_i) \quad (A.4)$$

$$BTmean(x_i) = -0.48 + 1.03 \times ATmean(x_i) \quad (A.5)$$

$$BTmax(x_i) = 0.03 + 0.99 \times ATmax(x_i) \quad (A.6)$$

Effective bark temperature (BTeff) between the lower development threshold (DT_L = 7.4°C) and optimum temperature (T_O = 30.0°C) was calculated with a linear function (A.7). Effective bark temperature between T_O and the upper development threshold (DT_U = 39.4°C) was calculated with a non-linear function (Eq. (5); (A.8)). For bark temperatures outside the lower and upper temperature thresholds ($BT \leq DT_L$ and $BT \geq DT_U$), BTeff was set to zero (A.9). Three variants of BTeff were calculated with Eqs. (A.4)–(A.6).

$$\text{If } BT(x_i) > DT_L \text{ and } BT(x_i) \leq T_O \; BTeff(x_i) = BT(x_i) - 7.4 \quad (A.7)$$

$$\text{If } BT(x_i) > T_O \text{ and } BT(x_i) < DT_U \; BTeff(x_i) = (T_O - DT_L) \times (\exp(\alpha \times BT) - \exp(\alpha \times T_{max} - (T_{max} - BT)/\beta) - \gamma), \text{ where } \alpha = 0.031;\ \beta = 5.3;\ \gamma = 1.25;\ T_{max} = 41.97 \quad (A.8)$$

If $BT \leq DT_L$ or $BT(x_i) \geq DT_U$ $BTeff(x_i) = 0$ (A.9)

A.2. Phenology model of *P. chalcographus*

CHAPY comprises following stepwise computations for any location (grid cell x):

- Calculation of the year day of onset of swarming ($YD_{swarming}$) based on the threshold for flight activity and on cumulative daily maximum air temperatures (ATmax) above the DT_L from 9th March onwards:

$YD_{swarming}$ if ATmax > 15.6°C and $\sum$(ATmax – 7.4) ≥ 80.5 dd (A.10)

- Calculation of the year day of the onset of infestation ($YD_{infestation}$) based on the threshold for flight activity and on cumulative daily maximum air temperatures (ATmax) above the DT_L from 9th March onwards:

$YD_{infestation}$ if ATmax > 15.6°C and $\sum$(ATmax – 7.4) ≥ 216.5 dd (A.11)

- Calculation of the cumulative sum of effective bark temperature (BTeff) relative to the necessary thermal sum for total development (K = 635.4 dd) of the parental generation:

if $YD \geq YD_{infestation}$ $Tsum_{F1} = K^{-1} \times \sum BTeff$ (A.12)

- Calculation of the onset of sister broods and their cumulative sum of effective bark temperatures (BTeff) relative to the thermal sum required for total development (K = 635.4 dd) of the sister brood:

$YD_{sister\ brood}$ if $Tsum_{F1}$ > 0.5 and ATmax > 15.6°C and daylength ≥ 13.6 h

if $YD \geq YD_{sister\ brood}$ $Tsum_{sister\ brood} = K^{-1} \times \sum BTeff$ (A.13)

- Calculation of the onset of the second, third and also possibility of a fourth filial generation and their cumulative sum of effective bark temperatures (BTeff) relative to the thermal sum required for total development (K = 635.4 dd):

YD_{F2} if $Tsum_{F1}$ > 1 and ATmax > 15.6°C and daylength ≥ 13.6 h

if $YD \geq YD_{F2}$ $Tsum_{F2} = K^{-1} \times \sum BTeff$ (A.14)

YD_{F3} if $Tsum_{F1}$ > 2 and ATmax > 15.6°C and daylength ≥ 13.6 h

if $YD \geq YD_{F3}$ $Tsum_{F3} = K^{-1} \times \sum BTeff$ (A.15)

YD_{F4} if $Tsum_{F1}$ > 3 and ATmax > 15.6°C and daylength ≥ 13.6 h

if $YD \geq YD_{F4}$ $Tsum_{F4} = K^{-1} \times \sum BTeff$ (A.16)

Finally, the relative thermal sum of each initiated generation at the end of December of each year and of each grid cell is evaluated for its probability of survival during the cold period. Since the adult stage is the most widespread overwintering stage (Koštál *et al.*, 2014), it is assumed that preimaginal stages of *P. chalcographus* do not survive winter. At relative thermal sums higher than 80% of the necessary thermal sum for total development ($Tsum_{Fx} \geq 0.8$), the initiated generation has completed its preimaginal development and can successfully hibernate as young adults. Therefore, initiated generations with relative thermal sums < 0.8 are ignored for calculating the total number of potential generations per year. Furthermore, the model is calculated only for grid cells containing appropriate host trees (Norway spruce) for *P. chalcographus*.

References

Anderbrant, O., Löfqvist, J., 1988. Relation between first and second brood production in the bark beetle *Ips typographus* (Scolytidae). Oikos 53, 357-365. https://doi.org/10.2307/3565536

Avtziz, D.N., Arthofer, W., Stauffer, C., Avtzis, N., Wegensteiner, R., 2010. *Pityogenes chalcographus* (Coleoptera: Scolytinae) at the southernmost borderline of Norway spruce (*Picea abies*) in Greece. Entomol. Hell. 19, 3-13. http://dx.doi.org/10.12681/eh.11589

Baier, P., Pennerstorfer, J., Otto, L.-F., Schopf, A., 2012. Online-Modellierung der Entwicklung und der Phänologie des Buchdruckers (*Ips typographus*) auf Basis des Modells PHENIPS und täglicher Wetter-und Prognosedaten des DWD. Mitt. Dtsch. Ges. allg. angew. Entomol. 18, 397-400.

Baier, P., Pennerstorfer, J., Schopf, A., 2007. PHENIPS—A comprehensive phenology model of *Ips typographus* (L.) (Col., Scolytinae) as a tool for hazard rating of bark beetle infestation. For. Ecol. Manage. 249, 171–186. https://doi.org/10.1016/j.foreco.2007.05.020

Berec, L., Doležal, P., Hais, M., 2013. Population dynamics of *Ips typographus* in the Bohemian Forest (Czech Republic): Validation of the phenology model PHENIPS and impacts of climate change. For. Ecol. Manage. 292, 1-9. http://dx.doi.org/10.1016/j.foreco.2012.12.018

Bertheau, C., Bankhead-Dronnet, S., Martin, C., Lieutier, F., Roux-Morabito, G., 2012. Lack of genetic differentiation after host range extension argues for the generalist nature of *Pityogenes chalcographus* (Curculionidae: Scolytinae). Ann. For. Sci. 69, 313-323. http://dx.doi.org/10.1007/s13595-011-0161-4

Bertheau, C., Salle, A., Roux-Morabito, G., Garcia, J., Certain, G., Lieutier, F., 2009. Preference–performance relationship and influence of plant relatedness on host use by *Pityogenes chalcographus* L. Agric. For. Entomol. 11, 389-396. http://dx.doi.org/10.1111/j.1461-9563.2009.00442.x

Coeln, M., Niu, Y., Führer, E., 1996. Temperature-related development of spruce bark beetles in montane forest formations (Coleoptera: Scolytidae). Entomol. Gener. 21, 37-54. http://dx.doi.org/10.1127/entom.gen/21/1996/37

Damos, P., Savopoulou-Soultani, M., 2012. Temperature-driven models for insect development and vital thermal requirements. Psyche 2012, 13. http://dx.doi.org/10.1155/2012/123405

Davídková, M., Doležal, P., 2017. Sister broods in the spruce bark beetle, *Ips typographus* (L.). For. Ecol. Manage. 405, 13-21. https://doi.org/10.1016/j.foreco.2017.08.040

Davídková, M., Doležal, P., 2019. Temperature-dependent development of the double-spined spruce bark beetle *Ips duplicatus* (Sahlberg, 1836) (Coleoptera; Curculionidae). Agric. For. Entomol. 21, 388-395. http://dx.doi.org/10.1111/afe.12345

de Groot, M., Ogris, N., 2019. Short-term forecasting of bark beetle outbreaks on two economically important conifer tree species. For. Ecol. Manage. 450, 117495. https://doi.org/10.1016/j.foreco.2019.117495

de Groot, M., Ogris, N., Kobler, A., 2018. The effects of a large-scale ice storm event on the drivers of bark beetle outbreaks and associated management practices. For. Ecol. Manage. 408, 195-201. https://doi.org/10.1016/j.foreco.2017.10.035

Depinay, J.-M.O., Mbogo, C.M., Killeen, G., Knols, B., Beier, J., Carlson, J., Dushoff, J., Billingsley, P., Mwambi, H., Githure, J., Toure, A.M., Ellis McKenzie, F., 2004. A simulation model of African Anopheles ecology and population dynamics for the analysis of malaria transmission. Malar. J. 3, 29. http://dx.doi.org/10.1186/1475-2875-3-29

Faccoli, M., Stergulc, F., 2004. *Ips typographus* (L.) pheromone trapping in south Alps: spring catches determine damage thresholds. J. Appl. Entomol. 128, 307-311. https://doi.org/10.1111/j.1439-0418.2004.00848.x

Faccoli, M., Stergulc, F., 2006. A practical method for predicting the short-time trend of bivoltine populations of *Ips typographus* (L.) (Col., Scolytidae). J. Appl. Entomol. 130, 61–66. https://doi.org/10.1111/j.1439-0418.2005.01019.x

Fahse, L., Heurich, M., 2011. Simulation and analysis of outbreaks of bark beetle infestations and their management at the stand level. Ecol. Model. 222, 1833-1846. https://doi.org/10.1016/j.ecolmodel.2011.03.014

Führer, E., Chen, Z.Y., 1979. Zum Einfluß von Photoperiode und Temperatur auf die Entwicklung des Kupferstechers, *Pityogenes chalcographus* L. (Col., Scolytidae). Eur. J. For. Res. 98, 87-91. http://dx.doi.org/10.1007/bf02743103

GIS, ZGS, 2020. Database of Forest Protection: monitoring of spruce bark beetles in pheromone traps and trap trees. Slovenian Forestry Institute, Slovenia Forest Service, Ljubljana.

Göthlin, E., Schroeder, L.M., Lindelöw, A., 2000. Attacks by *Ips typographus* and *Pityogenes chalcographus* on windthrown spruces (*Picea abies*) during the two years following a storm felling. Scand. J. For. Res. 15, 542-549. http://dx.doi.org/10.1080/028275800750173492

Haiden, T., Kann, A., Wittmann, C., Pistotnik, G., Bica, B., Gruber, C., 2011. The Integrated Nowcasting through Comprehensive Analysis (INCA) System and Its Validation over the Eastern Alpine Region. Weather Forecast. 26, 166-183. https://doi.org/10.1175/2010WAF2222451.1

Harding, S., Lapis, E.B., Bejer, B., 1986. Observations on the activity and development of *Pityogenes chalcographus* L. (Col., Scolytidae) in stands of Norway spruce in Denmark. J. Appl. Entomol. 102, 237-244. http://dx.doi.org/10.1111/j.1439-0418.1986.tb00917.x

Hedgren, P.O., 2004. The bark beetle *Pityogenes chalcographus* (L.) (Scolytidae) in living trees: reproductive success, tree mortality and interaction with *Ips typographus*. J. Appl. Entomol. 128, 161-166. http://dx.doi.org/10.1046/j.1439-0418.2003.00809.x

Hedgren, P.O., Weslien, J., Schroeder, L.M., 2003. Risk of attack by the bark beetle *Pityogenes chalcographus* (L.) on living trees close to colonized felled spruce trees. Scand. J. For. Res. 18, 39-44. http://dx.doi.org/10.1080/02827581.2003.10383136

Heliövaara, K., Peltonen, M., 1999. Bark beetles in a changing environment. Ecological Bulletins, 48-53. https://www.jstor.org/stable/20113226

Hijmans, R.J., 2016. raster: Geographic Data Analysis and Modeling. R package version 2.5-8. https://CRAN.R-project.org/package=raster.

Iooss, B., Janon, A., Pujol, G., Broto, B., Boumhaout, K., Da Veiga, S., Delage, T., Fruth, J., Gilquin, L., Guillaume, J., Le Gratiet, L., Lemaitre, P., Marrel, A., Meynaoui, A., Nelson, B.L., Monari, F., Oomen, R., Rakovec, O., Ramos, B., Roustant, O., Song, E., Staum, J., Sueur, R., Touati, T., Weber, F., 2019. sensitivity: Global Sensitivity Analysis of Model Outputs. R package version 1.17.0. https://CRAN.R-project.org/package=sensitivity (accessed

Jansen, M.J.W., 1999. Analysis of variance designs for model output. Computer Physics Communications 117, 35-43. https://doi.org/10.1016/S0010-4655(98)00154-4

Jarošík, V., Honěk, A., Magarey, R.D., Skuhrovec, J., 2011. Developmental database for phenology models: Related insect and mite species have similar thermal requirements. J. Econ. Entomol. 104, 1870-1876. http://dx.doi.org/10.1603/EC11247

Jarošík, V., Honěk, A., Magarey, R.D., Skuhrovec, J., 2012. PRATIQUE: Enhancements of pest risk analysis techniques. Data on thermal requirements for insects and mites (20/04/2012). https://secure.fera.defra.gov.uk/pratique/downloadItem.cfm?id=491 (accessed 14/12/2018)

Jurc, M., 2008. Gozdna zoologija. Univerza v Ljubljani, Biotehniška fakulteta, Oddelek za gozdarstvo in obnovljive gozdne vire, Ljubljana.

Jurc, M., Pavlin, R., Kavčič, A., de Groot, M., Hauptman, T., 2017. Recommendations for the use of various biotechnical methods and chemical agents for bark beetle control (Curculionidae: Scolytinae). Gozdarski vestnik 75, 94-111.

Kacprzyk, M., 2012. Feeding habits of *Pityogenes chalcographus* (L.) (Coleoptera: Scolytinae) on Norway Spruce (*Picea abies*) L. (Karst.) logging residues in wind-damaged stands in southern Poland. Int. J. Pest Manag. 58, 121-130. http://dx.doi.org/10.1080/09670874.2012.669077

Kacprzyk, M., Bednarz, B., 2015. The possibilities of six-toothed bark beetle (*Pityogenes chalcographus* L.) (Coleoptera: Scolytinae) sex identification based on adults' biometric characteristic. J. Entomol. Res. Soc. 17, 71-82. http://www.entomol.org/journal/index.php/JERS/article/view/766

Kann, A., Pistotnik, G., Bica, B., 2012. INCA-CE: a Central European initiative in nowcasting severe weather and its applications. Adv. Sci. Res. 8, 67-75. https://doi.org/10.5194/asr-8-67-2012

Kasumović, L., 2016. Adaptive changes of life cycle, overwintering and spatial distribution of spruce bark beetles (*Ips typographus* L. and *Pityogenes chalcographus* L.) in relation with dominant habitat conditions. Faculty of Forestry, University of Zagreb, Zagreb.

Koštál, V., Miklas, B., Doležal, P., Rozsypal, J., Zahradníčková, H., 2014. Physiology of cold tolerance in the bark beetle, *Pityogenes chalcographus* and its overwintering in spruce stands. J. Insect Physiol. 63, 62-70. https://doi.org/10.1016/j.jinsphys.2014.02.007

Kula, E., Ząbecki, W., 2006. Spruce windfalls and cambioxylophagous fauna in an area with the basic and outbreak state of *Ips typographus* (L.). J. For. Sci. 52, 497–509. http://dx.doi.org/10.17221/4530-JFS

Lactin, D.J., Holliday, N.J., Johnson, D.L., Craigen, R., 1995. Improved rate model of temperature-dependent development by arthropods. Environ. Entomol. 24, 68-75. http://dx.doi.org/10.1093/ee/24.1.68

Lekander, B., Lindelöw, Å., 1977. Helträdsutnyttjandet och insecterna. Department of Forest Entomology, Swedish University of Agricultural Sciences. PHU Rapport 52

Lobinger, G., 1994. Die Lufttemperatur als limitierender Faktor für die Schwärmaktivität zweier rindenbrütender Fichtenborkenkäferarten, *Ips typographus* L. und *Pityogenes chalcographus* L. (Col., Scolytidae). J. Pest Sci. 67, 14–17. https://doi.org/10.1007/BF01906563

Logan, J.A., Wollkind, D.J., Hoyt, S.C., Tanigoshi, L.K., 1976. An analytic model for description of temperature dependent rate phenomena in arthropods. Environ. Entomol. 5, 1133-1140. http://dx.doi.org/10.1093/ee/5.6.1133

Nagel, T.A., Firm, D., Rozenbergar, D., Kobal, M., 2016. Patterns and drivers of ice storm damage in temperate forests of Central Europe. Eur. J. For. Res. 135, 519-530. https://doi.org/10.1007/s10342-016-0950-2

Ogris, N., 2012. Prognostic fundamentals for forest protection in Slovenia. Silva Slovenica, Ljubljana. https://www.zdravgozd.si/dat/gradivo/16.pdf

Ogris, N., 2017a. Fenološki model za osmerozobega smrekovega lubadarja (*Ips typographus*) RITY-1 na območju Slovenije. Napovedi o zdravju gozdov 2017. https://doi.org/10.20315/NZG.33

Ogris, N., 2017b. Prostorski prikaz razvoja osmerozobega smrekovega lubadarja (*Ips typographus*) na območju Slovenije. Novice iz varstva gozdov 10, 3–7. https://doi.org/10.20315/NVG.10.2

Ogris, N., 2018a. Spletna aplikacija za izračun fenološkega modela za osmerozobega smrekovega lubadarja (*Ips typographus*) RITY-2. Napovedi o zdravju gozdov 2018. https://doi.org/10.20315/NZG.48

Ogris, N., 2018b. Spletna aplikacija za prostorski prikaz razvoja osmerozobega smrekovega lubadarja (*Ips typographus*), model RITY-2. Napovedi o zdravju gozdov 2018. https://doi.org/10.20315/NZG.49

Ogris, N., 2019a. Source code for Microsoft SQL Server T-SQL stored procedure for a point based queries of the phenology CHAPY-1 model of *Pityogenes chalcographus*. https://www.zdravgozd.si/projekti/podlubniki/doc/chapy_xy.zip (accessed 28. July 2019)

Ogris, N., 2019b. Source code for the raster based phenology CHAPY-1 model of *Pityogenes chalcographus* for use with Microsoft Visual Studio. https://www.zdravgozd.si/projekti/podlubniki/doc/chapy_raster.zip (accessed 28. July 2019)

Ogris, N., 2019c. Spletna aplikacija za izračun fenološkega modela za šesterozobega smrekovega lubadarja (*Pityogenes chalcographus*), model CHAPY-1. Napovedi o zdravju gozdov 2019. http://dx.doi.org/10.20315/NZG.45

Ogris, N., 2019d. Spletna aplikacija za prostorski prikaz razvoja šesterozobega smrekovega lubadarja (*Pityogenes chalcographus*), model CHAPY-1. Napovedi o zdravju gozdov 2019. http://dx.doi.org/10.20315/NZG.46

Ogris, N., 2020. Forest protection, computer application, v3.0. Slovenian Forestry Institute, Ljubljana.

Ogris, N., Ferlan, M., Hauptman, T., Pavlin, R., Kavčič, A., Jurc, M., De Groot, M., 2019. RITY – A phenology model of *Ips typographus* as a tool for optimization of its monitoring. Ecol. Model. 410, 108775. https://doi.org/10.1016/j.ecolmodel.2019.108775

Ogris, N., Jurc, M., 2010. Sanitary felling of Norway spruce due to spruce bark beetles in Slovenia: a model and projections for various climate change scenarios. Ecol. Model. 221, 290–302. https://doi.org/10.1016/j.ecolmodel.2009.05.015

Otero, M., Schweigmann, N., Solari, H.G., 2008. A stochastic spatial dynamical model for *Aedes aegypti*. Bull. Math. Biol. 70, 1297. http://dx.doi.org/10.1007/s11538-008-9300-y

R Core Team, 2018. R: A language and environment for statistical computing. R Foundation for Statistical Computing, Vienna, Austria. https://www.R-project.org/.

Ripley, B., Lapsley, M., 2017. RODBC: ODBC Database Access. RODBC: ODBC Database Access. R package version 1.3-15. https://CRAN.R-project.org/package=RODBC.

RS, 2009. Rules on forest protection. The Official Gazette of the Republic of Slovenia, 114/09 and 31/16. http://www.pisrs.si/Pis.web/pregledPredpisa?id=PRAV9492

Saltelli, A., Annoni, P., Azzini, I., Campolongo, F., Ratto, M., Tarantola, S., 2010. Variance based sensitivity analysis of model output. Design and estimator for the total sensitivity index. Computer Physics Communications 181, 259-270. https://doi.org/10.1016/j.cpc.2009.09.018

Schroeder, L.M., 2013. Monitoring of *Ips typographus* and *Pityogenes chalcographus*: influence of trapping site and surrounding landscape on catches. Agric. For. Entomol. 15, 113-119. http://dx.doi.org/10.1111/afe.12002

Schwerdtfeger, F., 1929. Ein Beitrag zur Fortpflanzungsbiologie des Borkenkäfers *Pityogenes chalcographus* L. J. Appl. Entomol. 15, 335-427. https://doi.org/10.1111/j.1439-0418.1929.tb00113.x

Signorell, A., et mult. al., 2018. DescTools: Tools for descriptive statistics. R package version 0.99.26. URL: https://cran.r-project.org/package=DescTools.

Sobol', I.M., 1993. Sensitivity analysis for non-linear mathematical models. Mathematical Modelling and Computational Experiment 1, 407-414.

Štefková, K., Okrouhlík, J., Doležal, P., 2017. Development and survival of the spruce bark beetle, *Ips typographus* (Coleoptera: Curculionidae: Scolytinae) at low temperatures in the laboratory and the field. Eur. J. Entomol. 114, 1-6. https://doi.org/10.14411/eje.2017.001

Verkaik, E., Moraal, L.G., Nabuurs, G.J., 2009. Potential impacts of climate change on Dutch forests, mapping the risks. Alterra, Wageningen.

Wermelinger, B., Seifert, M., 1998. Analysis of the temperature dependent development of the spruce bark beetle *Ips typographus* (L.) (Col., Scolytidae). J. Appl. Entomol. 122, 185-191. https://doi.org/10.1111/j.1439-0418.1998.tb01482.x

Wermelinger, B., Seifert, M., 1999. Temperature-dependent reproduction of the spruce bark beetle *Ips typographus*, and analysis of the potential population growth. Ecol. Entomol. 24, 103-110. https://doi.org/10.1046/j.1365-2311.1999.00175.x

ZGS, 2018a. Načrt sanacije gozdov, poškodovanih v vetrolomu od 11. do 13. decembra 2017. Zavod za gozdove Slovenije, Ljubljana.

ZGS, 2018b. Poročilo Zavoda za gozdove Slovenije o gozdovih za leto 2017. Zavod za gozdove Slovenije, Ljubljana. http://www.zgs.si/fileadmin/zgs/main/img/PDF/LETNA_POROCILA/2017_Porocilo_o_gozdovih.PDF

ZGS, 2018c. Timber. Database about felling in Slovenia. Slovenia Forest Service

Zúbrik, M., Raši, R., Vakula, J., Varínsky, J., Nikolov, C., Novotný, J., 2008. Bark beetle (*Ips typographus* L., *Pityogenes chalcographus* L., Col.: Scolytidae) pheromone traps spatial distribution optimisation in central Slovakian mountains. Lesnícky časopis 54, 235-248.

Zumr, V., 1982. The data for the prognosis of spring swarming of main species of bark beetles (Coleoptera, Scolytidae) on the spruce (*Picea excelsea* L.). J. Appl. Entomol. 93, 305-320. http://dx.doi.org/10.1111/j.1439-0418.1982.tb03600.x

Zumr, V., Soldan, T., 1981. Reproductive cycles of *Ips typographus*, *Ips amitinus* and *Pityogenes chalcographus (C*oleoptera: Scolytidae). Eur. J. Entomol. 78, 280-289.

Zupančič, M., Marinček, L., Seliškar, A., Puncer, I., 1987. Considerations on the phytogeographic division of Slovenia. Biogeographia 13, 89–98. http://dx.doi.org/10.21426/B613110276

Supplemental materials

Table S1. (a) Re-emergence of *Pityogenes chalcographus* parental beetles and relative thermal sum at the time of re-emergence according to daily observed bark temperatures; (b) Observed and predicted thermal sum needed for development of filial beetles, observed and estimated emergence of filial beetles, and deviation of estimated emergence from observed data (MAE: mean absolute error of estimated emergence of filial beetles)

			(a) Re-emergence		(b) Development of filial beetles				
Location	Temperature of growth chamber (°C)	Observed onset of infestation [a]	Date	Relative thermal sum (%) [b]	Observed thermal sum (dd)	Estimated thermal sum (dd)	Observed emergence of filial beetles	Predicted emergence of filial beetles	Deviation (days)
Vodice	23	10/04/2017	22/06/2017	71.7	675.4	639.2	04/07/2017	04/07/2017	0
Vodice	28	10/04/2017	20/06/2017	66.5	606.1	569.9	28/06/2017	02/07/2017	4
Kamnik	23	03/04/2017	13/06/2017	56.1	627.8	609.8	28/06/2017	30/06/2017	2
Kamnik	28	03/04/2017	13/06/2017	56.1	642.2	624.1	26/06/2017	27/06/2017	1
Brode	23	10/04/2017	28/06/2017	59.6	615.7	721.5	11/07/2017	06/07/2017	–5
Brode	28	10/04/2017	28/06/2017	60.2	729.7	835.5	14/07/2017	05/07/2017	–9
Prevala	23	29/05/2017	11/07/2017	67	649.6	684	24/07/2017	22/07/2017	–2
Prevala	28	29/05/2017	13/07/2017	73.4	618	652.4	20/07/2017	20/07/2017	0
Medvedica	28	25/04/2018	29/06/2018	83.3	650	578.1	04/07/2018	07/07/2018	3
Medvedica	28	02/05/2018	29/06/2018	75.8	661.1	598	07/07/2018	09/07/2018	2
Medvedica	28	09/05/2018	01/07/2018	75.3	634.5	579.9	08/07/2018	11/07/2018	3
Turjak	23	02/05/2018	30/06/2018	68.9	652.4	639.1	12/07/2018	12/07/2018	0
Turjak	28	02/05/2018	28/06/2018	58.3	631.6	618.3	08/07/2018	09/07/2018	1
Turjak	28	09/05/2018	28/06/2018	64.4	590.3	579.9	08/07/2018	11/07/2018	3
Erjavčev laz	23	25/04/2018	28/06/2018	84.7	736.1	631.6	09/07/2018	10/07/2018	1
Erjavčev laz	28	25/04/2018	28/06/2018	85.4	743.3	638.9	07/07/2018	07/07/2018	0
Erjavčev laz	28	02/05/2018	28/06/2018	76.4	684.3	598	07/07/2018	09/07/2018	2
Mokrc [c]	28	25/04/2018	28/06/2018	62.4	602.7	638.9	07/07/2018	07/07/2018	0
			Mean	69.2	652.8	635.4		MAE	2.1
			95% conf. int.	4.8	22.7	31.4			
			Minimum	56.1	590.3	569.9			–9.0
			Maximum	85.4	743.3	835.5			4

[a] Sample chunks from same location with different onsets of infestation

[b] Relative thermal sum expressed as a percentage of the thermal sum required for total development (observed from daily data: 652.8 dd)

[c] At location Mokrc two chunks were removed from the trap log, but only one was successfully infested.

Demonstration of the phenology model CHAPY

Using the daily data output of the INCA system, the timing of the key-phenological events in the bark beetle life cycle was simulated for the study area with the modelling procedures of CHAPY (see Eqs. (A.10)–(A.15)). These include the (1) onset of swarming; (2) onset of infestation (start of development); (3) cumulative sum of effective bark temperature of parental, sister and filial generations; and finally (4) total number of generations.

The accuracy of our model in estimating bark beetle phenology is demonstrated by comparison between the observed and predicted developmental stage of the beetles in trap trees at the two selected sites of Vodice in 2017 and Medvedica in 2018 (**Fig. S.1**). The first site is located in a lowland area (330 m a.s.l.), and the second site is located in the Dinaric Alps at an altitude of 426 m and WNW aspect (Table 1).

Using INCA estimated air temperature for analysis of bark beetle development at trap trees, the estimated thermal sum at the time of emergence showed a lower variability than that calculated with hourly recorded data. However, the mean value calculated from the INCA system was not significantly different from the required thermal sum for total development (test value $K = 598$ dd) and deviated by 6.9 dd (Table 4).

At the Vodice location, the CHAPY model predicted two filial broods and two sister brood (**Fig. S.1**). Both filial broods and the first sister brood completed the total development cycle. However, the second sister brood reached 66% of the relative thermal sum required for total development by the end of December 2017, indicating the late larvae developmental stage. Since the second sister brood did not exceed 80% of relative thermal sum required for total development, the model assumed that this brood would not successfully overwinter. The predicted onset of swarming was three days earlier than observed and onset of infestation matched the observed date.

The model predicted two filial broods and two sister broods at the higher elevation location at Medvedica (**Fig. S.1**). Both filial broods and the first sister brood achieved 100% of the thermal sum required for total development. The second sister brood reached 64% of the relative thermal sum required for total development by the end of December 2018, indicating the late larvae developmental stage. No additional brood was laid after 25th August due to the daylength limitation (< 13.6 h). The predicted onset of swarming was six days later than observed, and the predicted onset of infestation was four days earlier than observed.

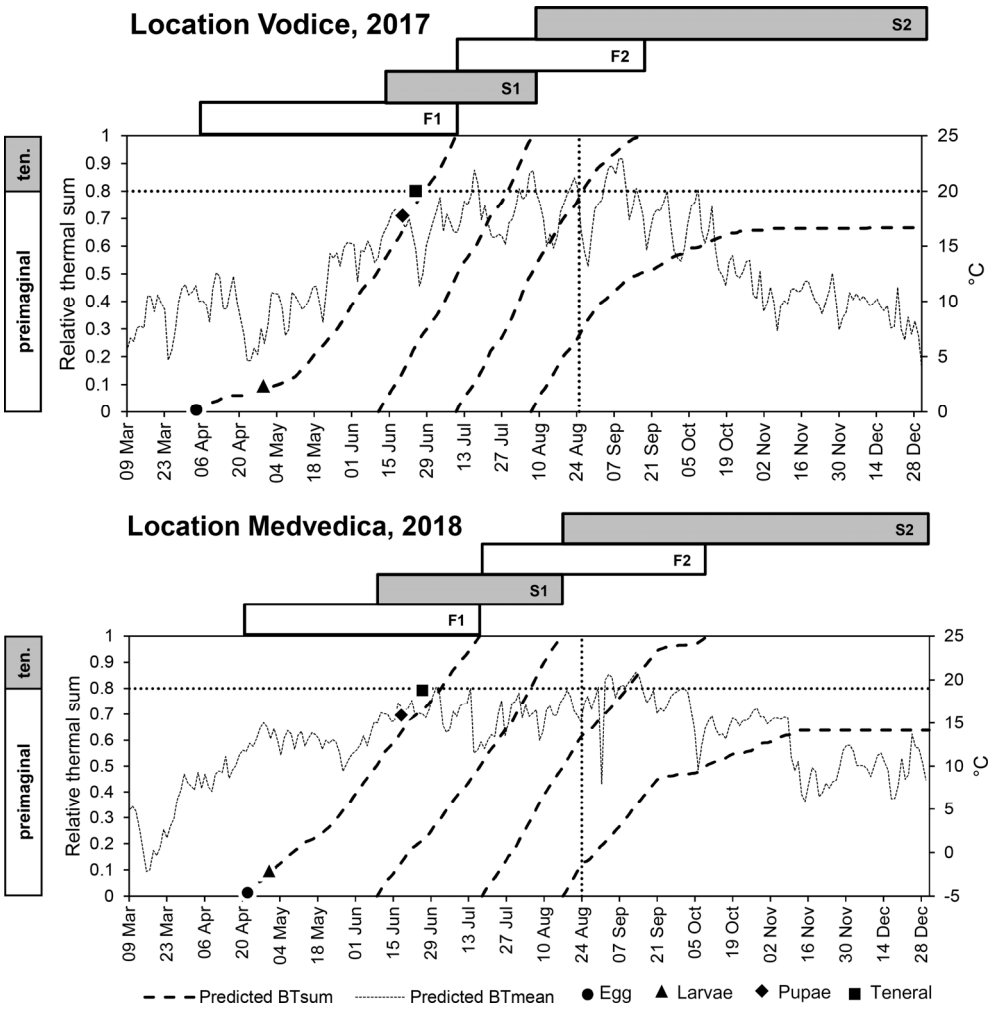

Fig. S.1. Time series of estimated daily mean bark temperature (BTmean), relative thermal sums of the predicted development of *P. chalcographus* using INCA temperature data at two selected locations according to the AVG scenario. Development of a new generation starts at the predicted onset of infestation. The dotted horizontal line marks the threshold for successful hibernation (relative thermal sum ≥ 0.8); the dotted vertical line indicates the threshold for induction of diapause (daylength = 13.6 h); boxes illustrate potential generations (F = filial, S = sister brood); markers show observed events: circle – egg, triangle – larvae, diamond – pupae, square – teneral adult.

The point-based comparison revealed high conformity between the phenological events predicted by the model at the local trap log. This indicates the possibility to precisely compute local temperature conditions inside the bark with the model. The higher deviations between observed and predicted events might be due to uncertainties in weekly control intervals, the relatively small sample, and variability in beetle life processes that are not temperature dependent. However, the application of CHAPY using the INCA data can detect relevant differences in the phenology of *P. chalcographus*.

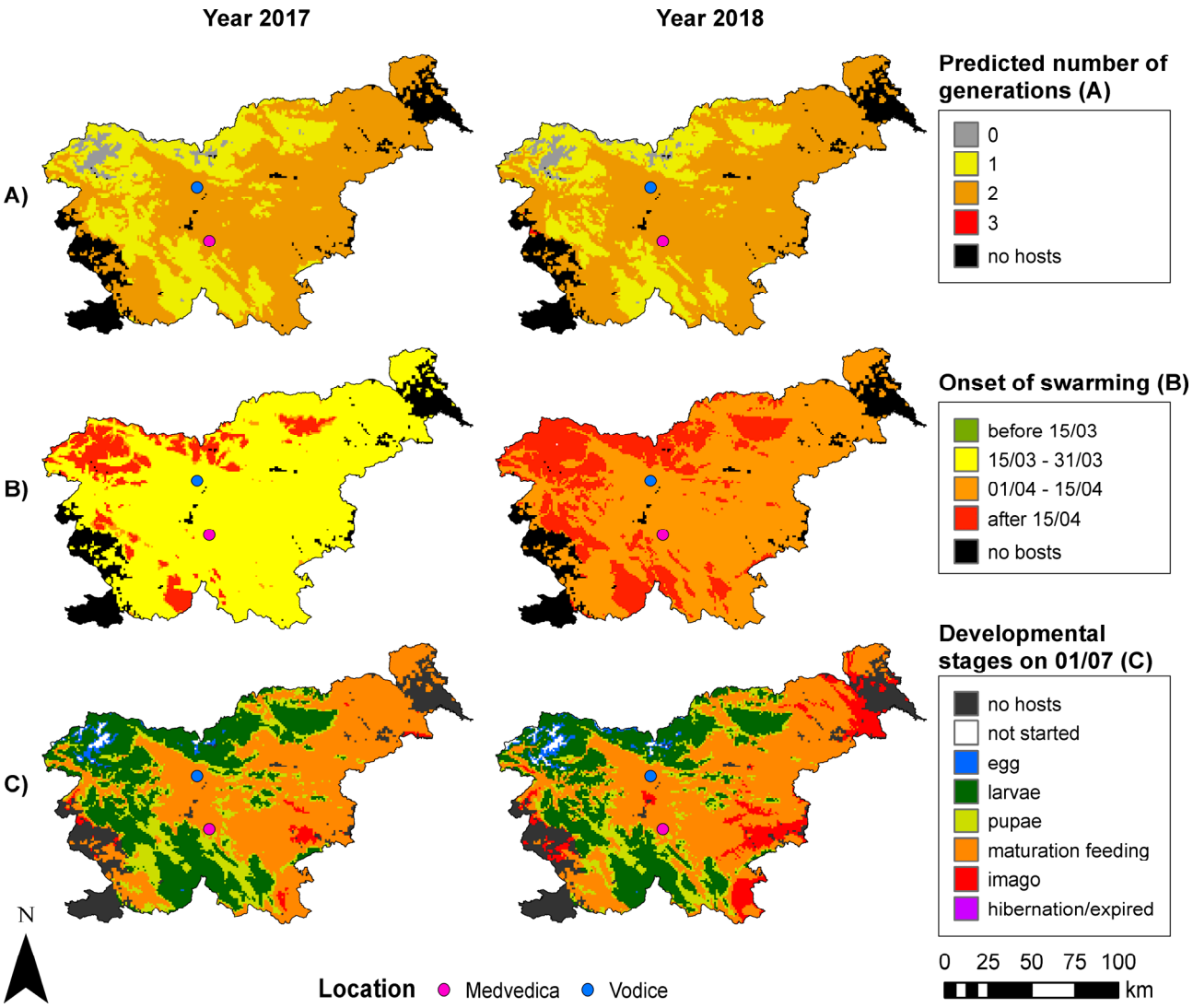

Fig. S.2. Predicted number of generations (A), onset of swarming (B) and developmental stages on 01/07 (C) for 2017 and 2018 in Slovenia according to the AVG scenario. Pink and blue dot depict two locations from Fig. S.1.

The onset of swarming in 2017 was most frequently predicted (86.7% of the area) between 15/03 and 31/03 (**Fig. S.2**B). In 2018 the onset of swarming was initiated later in the season. Between 01/04 and 15/04/2018, the predicted onset of swarming occurred on 74.2% of the model area. The onset of swarming did not occur before 15/03 in either 2017 or 2018. After 15/04/2018, the predicted onset of swarming occurred on 25.8% of the model area of (**Fig. S.2**B).

The model enables the spatial prediction of developmental stages for any point of time. **Fig. S.2** (C) shows an example for 01/07 for both 2017 and 2018. The most prevalent developmental stage of the first filial generation on 01/07 was estimated by the model to be the teneral adult (maturation feeding) stage, at 51.0% and 49.8% of the model area in 2017 and 2018, respectively. The imago stage was predicted on 1.4% and 8.6% of the model area in 2017 and 2018, respectively (**Fig. S.2**C).

The development rate was calculated with the MIN, AVG and MAX scenarios according to the three effective bark temperatures (Eqs. (A.4)–(A.6) and (A.7)–(A.9)). There were distinct differences in the predicted number of filial generations per year given by the different scenarios. In the MIN scenario, only one generation per year was prevalent in both 2017 and 2018 (**Fig. S.3**). However, in the MIN scenario in 2018, two generations of *P. chalcographus* were already present on 16.3% of the model area with appropriate hosts, whereas in 2017, two generations were completed on only 0.9% of the model area. In the AVG scenario, two filial generations were completed on 66.0% and 73.2% of the model area in 2017 and 2018, respectively (**Fig. S.2**A and

Fig. S.3). Up to three generations per year were predicted by the AVG scenario in 2018; however, three generations were completed on only 0.1% of the model area. In the MAX scenario, four generations per year were frequently predicted by the model, but three generations were prevalent in this scenario. In the MAX scenario, the thermal sum required for the completion of three generations accumulated on 68.4% and 74.0% of the model area in 2017 and 2018, respectively (**Fig. S.3**).

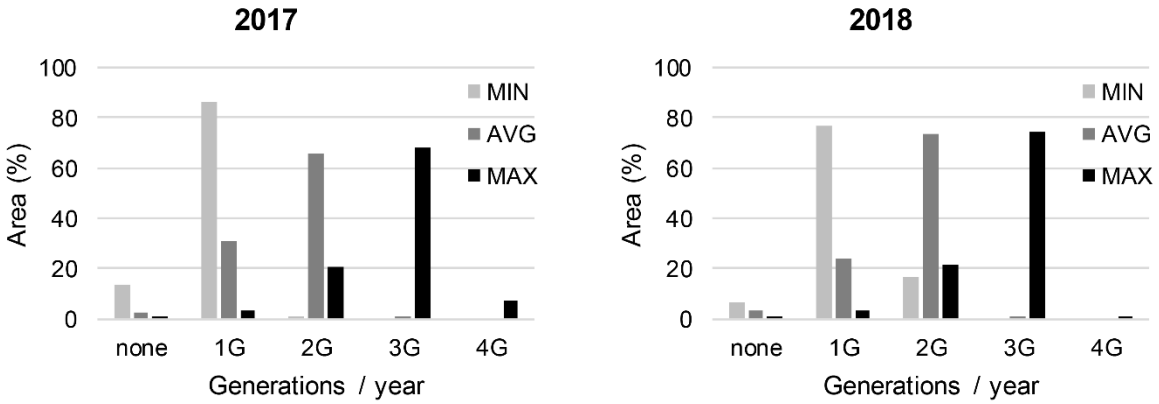

Fig. S.3. Relative area occupied by different numbers of predicted generations in 2017 and 2018 according to the MIN, AVG and MAX temperature scenarios